ACS ORGANIC & INORGANIC Au
AN OPEN ACCESS JOURNAL OF THE AMERICAN CHEMICAL SOCIETY



pubs.acs.org/orginorgau
Article

# Modeling of Optical Band-Gap Values of Mixed Oxides Having Spinel Structure $AB_2O_4$ (A = Mg, Zn and B = Al, Ga) by a Semiempirical Approach

Francesco Di Quarto,* Andrea Zaffora, Francesco Di Franco, and Monica Santamaria

Cite This: *ACS Org. Inorg. Au* 2024, 4, 120−134
Read Online



**ABSTRACT:** Spinel oxides with the general formula $AB_2O_4$ comprise a large family of compounds covering a very wide range of band-gap values (1 eV < $E_g$ < 8 eV) as a function of the nature of the metallic cations A and B. Owing to this, the physical properties of these materials have been largely exploited both from a fundamental point of view, for their variable electronic properties, and for their possible use in numerous engineering applications. Herein, the modeling of $ZnAl_2O_4$, $ZnGa_2O_4$, $MgAl_2O_4$, and $MgGa_2O_4$ cubic spinel oxides has been carried out by using the semiempirical approach based on the difference of electronegativity between oxygen and the average electronegativity of cations present in the oxides. The results of recent theoretical extensions of our semiempirical approach to ternary and quaternary oxides have been tested for spinel oxides with metallic ions occupying both octahedrally and tetrahedrally coordinated sites in different ratios. A detailed analysis of the experimental band-gap values and comparison with the theoretically estimated values has been carried out for ternary $ZnAl_2O_4$, $ZnGa_2O_4$, $MgAl_2O_4$, and $MgGa_2O_4$ spinels as well as for double spinels $Mg(Al_{2x}Ga_{2-x})O_4$ and $Zn(Al_{2x}Ga_{2-x})O_4$, and quaternary mixed oxides $(Zn_xMg_{(1-x)})Al_2O_4$ and $(Zn_xMg_{(1-x)})Ga_2O_4$. The wide range of band-gap values reported in the literature for simple or double spinels has been related to the different preparation methods affecting the grain dimension of crystalline spinel samples as well as to the presence of crystallographic defects and/or impurities in the spinel matrix. The good agreement between experimental band-gap values and the theoretical ones strongly supports the use of our semiempirical approach in the area of band-gap engineering of new materials.

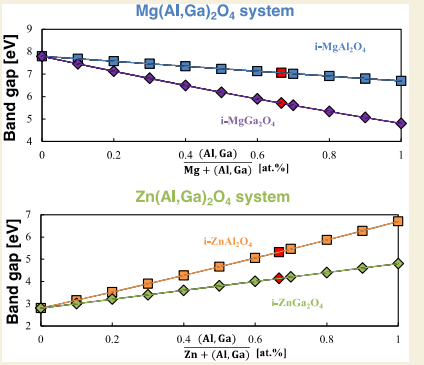


**KEYWORDS:** *spinel oxides, quaternary oxides, double spinels, band gap, band gap engineering*



## 1. INTRODUCTION

Numerous studies have been devoted to the fabrication and characterization of spinel oxides with general formula $AB_2O_4$ covering a very wide range of band-gap values (1 eV < $E_g$ < 8 eV) as a function of the nature of the metallic cations A and B. Owing to their wide spectrum of electronic and physical properties, spinel oxides have been investigated as possible candidates in numerous engineering applications as electro-photocatalysis, electroluminescence, optoelectronics, photonics and spintronics, energy conversion and storage, and as materials for the fabrication of resistive random access memories (RRAM) for low energy consumption in data storage applications.[1−8] Lower band-gap values ($E_g$ < 3.0 eV) have been reported for spinel oxides when the trivalent atom belongs to the transition d-metals, while highest band-gap values are, usually, reported for trivalent B atom belonging to the s,p-metal group (Al, Ga, In). Lower band-gap spinels have been largely investigated as possible photocatalysts and/or electrocatalysts in a photo-assisted water-splitting reaction and for an electrochemical oxygen evolution/reduction reaction (OER/ORR).[1−3] High band-gap spinels ($E_g$ > 3.0 eV) are of large interest for many relevant applications pertaining to the fields of electro-luminescence, electronics, photonics, and energy conversion, including, possibly, future fusion energy devices.[4,5,7,8] More specifically, $ZnAl_2O_4$ and $MgAl_2O_4$ spinel oxide systems are currently intensively investigated in the luminescence research area as possible phosphor candidates to substitute rare-earth-based alumina and gallia garnets,[9] as well as catalytic support or active materials in photocatalytic processes.[2,8] On the other hand, $MgAl_2O_4$ is also an interesting material for nuclear technologies as inert matrices for nuclear fuels or nuclear waste immobilization and as optical windows in fusion reactors and/or future fusion devices.[7] $ZnGa_2O_4$ has been investigated as photocatalytic material for the generation of molecular hydrogen, both under ultraviolet (UV) (250 nm) and under visible light (420 nm) as mixed spinel $ZnFeGaO_4$.[3] It is currently under

Received: July 15, 2023
Revised: November 2, 2023
Accepted: November 3, 2023
Published: November 21, 2023

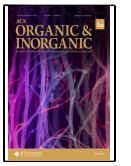

investigation as a wide-band-gap power oxide semiconductor and as "a promising energy electronic platform for futuristic energy generation, storage, and power system integration".[4] The electronic properties of $MgGa_2O_4$ spinel have been investigated owing to its use as a material for application in optoelectronics and spintronics and, very recently,[5] as a potential material for the fabrication of low energy consumption resistive random access memory (RRAM).

In the cubic $AB_2O_4$ spinel structure, A, usually, represents a bivalent cation occupying crystallographic sites tetrahedrally coordinated to oxygen ions, and B represents a trivalent cation occupying crystallographic sites octahedrally coordinated to oxygen ions. As for the cation distribution between tetrahedral and octahedral sites, the spinel structure is defined as "normal spinel" if the bivalent cations occupy only tetrahedral sites and the trivalent cations only the octahedral ones. In several cases, however, it is possible to observe a total or partial inversion of site occupancy with bivalent A cations occupying octahedral sites and trivalent B cations occupying tetrahedral sites. In this case, the spinel is defined as an inverted spinel, with the $i$ symbol representing the inversion degree: $(0 \leq i \leq 1)$. For $i = 0$, we have the normal spinel, while for $i = 1$, we have all bivalent cations occupying octahedral sites while half of the trivalent cations stay in tetrahedral sites. For the $i$ value different from zero and 1, the spinel structure is defined as a complex spinel. We have to say that the degree of inversion, i.e., the value of the i parameter, as well as the experimental band-gap values reported in the literature for spinel oxides, strongly depends on the preparation routes[1] as well as on the experimental techniques of measure. This is particularly evident for the reported band-gap values where different procedures of band-gap determination and different definitions of band gap are currently employed (see Section 1.2). In the case of the optical band gap, further complications arise in the presence of possible crystallographic defects and chemical impurities originating within the forbidden gap of the investigated material, optically active acceptor or donor electronic states.

This study represents a continuation of our previous works[9−12] aimed to stress the importance of the crystallographic structure in determining the band-gap value of the investigated materials and how to account for these changes in the crystallographic structure to derive the band-gap value by our semiempirical approach. According to this, we will investigate in detail the band-gap dependence from the composition and structure of a selected group of high band-gap ternary spinel oxides $MgAl_2O_4$, $ZnAl_2O_4$, $MgGa_2O_4$, and $ZnGa_2O_4$; quaternary double spinel oxides $Mg(Al_xGa_{(2-x)})O_4$ and $Zn(Al_xGa_{(2-x)})O_4$; as well as the quaternary mixed oxides $Zn_xMg_{(1-x)}Al_2O_4$. The investigated systems present several advantages as follows:

(a) The electronic structure of the constituent binary oxides MgO, ZnO, $Al_2O_3$, and $Ga_2O_3$ suggests that their band gap is of charge-transfer type and does not present possible complications related to the presence of a partially filled d-shell and a variable oxidation state typical of cations belonging to transitional metals.

(b) Quite extensive experimental and theoretical data sets of the physicochemical properties, including band-gap values, have been reported in the literature for all binary oxides entering the investigated spinels.

(c) The band-gap values covered by the binary oxides present in the spinel structure cover a quite wide range of values, from about 3.0 eV to around 9.0 eV, so that it will be possible to carry out a reliable comparison between the $E_g$ values derived by our semiempirical approach and the experimental ones as well as those derived by density functional theory (DFT)-rooted theoretical models based on first-principles.[13]

### 1.1. Theoretical Aspects and Validation of the Model

In previous work,[11] we suggested that the experimental band-gap data of 30 metal oxides, belonging both to s,p- and d-metal groups, could be fitted according to the following equation

$$E_g = A(\chi_O - \chi_M)^2 + B \tag{1}$$

where $\chi_M$ and $\chi_O$ represent the electronegativity values of the metal and oxygen, respectively, in Pauling's scale,[14] and $A$ and $B$ are two constants derived from the experimental data fitting. The values

$$A_{s,p\text{-met}} = 2.17 \quad \text{and} \quad B_{s,p\text{-met}} = -2.71[\text{eV}] \tag{2a}$$

were obtained for s,p-metal (II and XIII−XV groups in the periodic table of the elements) oxides and for d-metal (III−XII groups) oxides:

$$A_{d\text{-met}} = 1.35 \quad \text{and} \quad B_{d\text{-met}} = -1.49[\text{eV}] \tag{2b}$$

In the same work, we derived, also, for $A$ and $B$ the following expressions

$$A = 2E_I, \quad \text{and} \quad B = 1/y[(D_{M-M} + yD_{O-O}) - R_{(MO_y)}]$$

where $E_I$ is the extraionic energy unit orbitally dependent, assumed[15] "to vary with hybridization configuration, i.e., with different atomic coordinations in different crystal structures", $y$ is the stoichiometric coefficient of the oxide $MO_y$, $D_{M-M}$ and $D_{O-O}$ are the bond energies of diatomic molecules in the gas phase, and $R_{(MO_y)}$ is the repulsive energy term, generally, expressed as

$$R_{(MO_y)} = U_{lattice} - U_{bond}$$

with $U_{bond}$ being assumed coincident with Madelung energy $U_M$ in the ionic limit.

More recently,[10] we extended the semiempirical approach to pseudoregular (mixed s,p−s,p or d,d-metal oxides) and nonregular (s,p,d-metal oxides) ternary oxides by taking, also, into account the possible changes of band-gap values for oxide systems presenting different polymorphs. In order to model the ternary oxide band gap, $E_{gT}$, as a function of the composition, we proposed to use as a starting equation the relationship

$$\begin{aligned} E_{gT} &= x_1E_{g,1}(\chi_{av}) + x_2E_{g,2}(\chi_{av}) \\ &= E_{g,2}(\chi_{av}) + x_1[E_{g,1}(\chi_{av}) - E_{g,2}(\chi_{av})] \end{aligned} \tag{3a}$$

with

$$\begin{aligned} E_{g1}(\chi_{av}) &= A_1(\chi_o - \chi_{av})^2 + B_1 \quad \text{and} \\ E_{g2}(\chi_{av}) &= A_2(\chi_o - \chi_{av})^2 + B_2 \end{aligned} \tag{3b}$$

where

$$\chi_{av} = x_1\chi_1 + x_2\chi_2 \quad \text{and} \quad x_1 + x_2 = 1 \tag{3c}$$

$x_i$ and $\chi_i$ represent the cationic fraction (in atom %) and Pauling's electronegativity parameter, respectively, of each metal $M_i$ present in the mixed oxides. $E_{g,1}$ and $E_{g,2}$ represent the band-gap values of pure binary oxides, assumed to follow one of the two previous correlations (sp−sp or d−d-metal) according to


https://doi.org/10.1021/acsorginorgau.3c00030
ACS Org. Inorg. Au 2024, 4, 120−134

**Table 1. Band-Gap Values of Normal Spinels ($i = 0$) Estimated by the Semiempirical Approach, $E_g^{th}$, Experimental Optical Gap Values $^{d,i}E_{exp}^{opt}$ Obtained by Tauc's Method (d: Direct; i: Indirect), Experimental Excitation Peak Energy Values of the Excitonic Gap $E_{exp}^{exc}$, Experimental Fundamental Band Gap, $E_f^{exp}$, Obtained (through eq 7) from $E_{exp}^{exc}$, and Theoretical $E_f^{th}$ Obtained (through eqs 6 and 7) from $E_g^{opt}$**

| phase | $E_g^{th}$ [eV] | $E_{exp}^{opt}$ [eV] | $E_{exp}^{exc}$ [eV] | $E_g$ (DFT) [eV] | $E_f^{exp}$ [eV] | $E_f^{th}$ [eV] |
|---|---|---|---|---|---|---|
| *n*-$MgAl_2O_4$ | 7.88 | 7.80−8.03 | 7.385−7.434[26,27] | 5.10−7.80[28−32] | 7.80−7.88[26,27] | |
| *n*-$ZnAl_2O_4$ | 6.67 | 3.80−5.15[33−35] $^{d}$6.05[25] | 6.9 ± 0.1[8,22−24] | 6.18−6.55[33,34,36] | 7.28 ± 0.1 6.62[25] | |
| *n*-$MgGa_2O_4$ | 5.67 | 5.03−5.15[37,38] | 5.41 ± 0.05[39−41] | 5.11[30] | 5.64[39−41] | |
| *n*-$ZnGa_2O_4$ | 4.67 | $^{i}$(4.55−4.67) $^{d}$(4.70−4.90)[4,37,41−50] | 4.80−5.05[40,41,51] | 4.57−4.90[33,36,52] | 5.12 ± 0.1 5.27[53] | 5.10 ± 0.1 |
| $ZnGa_{2}O_{4:Bi2\%}^{+3}$ | | 4.60[54] | 4.85[54] | | 5.04[54] | |
| $ZnGa_{2}O_{4:Eu2-4\%}^{+3}$ | | 4.90[48] | | | 5.36[48] | |

**Table 2. Band-Gap Values of Inverse Spinels ($i = 1$) and Complex Spinel ($0 < i < 1$) Estimated by the Semiempirical approach (This Work) or Experimentally Obtained**

| inversion degree *i* | $MgAl_2O_4$ [eV] | $MgGa_2O_4$ [eV] | $ZnAl_2O_4$ [eV] | $ZnGa_2O_4$ [eV] | refs |
|---|---|---|---|---|---|
| 1.0 | 7.054 | 5.70 | 5.32 | 4.14 | this work |
| | 5.51[28] | 2.63[30] | | | DFT |
| 0.50 | 7.47 | | | | this work |
| | 4.84[28] | | | | DFT |
| 0.44 | | 5.68 | | | this work |
| | | 5.63[39,40] | | | exp |
| 0.38[60] | 7.57 | | | | this work 60,(i) |
| 0.30 | | | | 4.51 | this work |
| | | | | 4.75[46] | 46 |
| 0.17 | | | | 4.58 | this work |
| | | | | 4.53[46] | 46 |
| 0.13 | 7.80 | | | 4.60 | this work |
| 0.12 | 7.84[27] | | | 4.70,[48] 4.60[42] | 27,48,42 |
| 0.04 | | | 6.62 | | this work |
| | | | 6.62[25] | | 25 |
| 0.0 | 7.90[27] | 5.67 | 6.67 | | 27 |
| | 7.88 | | | 4.67 | this work |
| | 5.80−5.11 | | | | 28,30 |

eqs 1 and 2. After substitution of eqs 3b and 3c in eq 3a and simple algebraic manipulations, we got the equation for a generic ternary oxide system as

$$E_{g,T}(\chi_{av}) = E_{g,2} + S_l x_1 + S_q x^2 + S_c x^3 \quad (4a)$$

where $E_{g,2}$ is the band gap of the pure oxide corresponding to $x_1 = 0$, and

$$S_l = 2A_2(\chi_O - \chi_2)(\chi_2 - \chi_1) + (B_1 - B_2) + (A_1 - A_2)(\chi_O - \chi_2)^2 \quad (4b)$$

$$S_q = 2(A_1 - A_2)(\chi_O - \chi_2)(\chi_2 - \chi_1) + A_2(\chi_1 - \chi_2)^2 \quad (4c)$$

$$S_c = (A_1 - A_2)(\chi_1 - \chi_2)^2 \quad (4d)$$

As for the modeling, according to eqs 3a−3d, of the optical band gap of the investigated mixed oxide crystallizing in the spinel structure, the general chemical formula, $AB_2O_4$, can be more effectively written as $(A_{1-i}B_i)^T[A_iB_{2-i}]^{Oct}O_4$, where $(A)^T[B_2]^{Oct}O_4$ and $(B)^T[AB]^{Oct}O_4$ represent the normal ($i = 0$) and the inverse spinel ($i = 1$), respectively. In the case of a normal spinel, $i = 0$, we can assume that $ZnAl_2O_4$ and $ZnGa_2O_4$ can be fitted by following the methodology described in our previous works[10,12] dealing with ternary oxide systems and by taking into consideration that, as for $Zn^{2+}$ in tetrahedral coordination, the *A* and *B* values to be used coincide with the values derived for d-metal oxide by assuming the EN value for Zn in Pauling's scale of $\chi_{Zn} = 1.60$.[9−12] By using eq 2b, a band-gap value of 3.37 eV is, in fact, obtained in very good agreement with the values of 3.30−3.40 eV reported in the literature for wurtzite ZnO (wtz-ZnO).[10] According to this, for ternary oxide systems $(Zn)^T[Al_2]^{Oct}O_4$ and $(Zn)^T[Ga_2]^{Oct}O_4$, in eqs 3a−3c, we will assume as $E_{g2}$ the band-gap value of wtz-ZnO ($E_{g2} = 3.37$ eV) with $A_2 = 1.35$ and $B_2 = -1.50$ eV and, by remembering that in normal spinel, all $Al^{3+}$ ions occupy octahedral sites, we will assume as $E_{g1}$ the optical band-gap value of $\alpha$-$Al_2O_3$, the only polymorph of alumina oxides satisfying such a condition.[16] According to the data of Table 1 in ref 10, we will use for $\alpha$-$Al_2O_3$ the usual value of −2.71 eV for *B* and the value of $A = 2.8025$ derived from eq 2b by using 8.50 eV as an optical band-gap value of $\alpha$-$Al_2O_3$, as discussed in ref 10. Analogously, as for the *n*-$ZnGa_2O_4$ spinel, we will assume for wtz-ZnO the *A* and *B* values reported above for d-metal oxides, while the values of $A = 2.22$ and of $B = -2.71$ eV will be assumed for $\alpha$-$Ga_2O_3$ ($E_{g,opt} = 5.30$ eV), as reported in Table 2 of ref 10.

At variance with ZnO, the band gap of magnesium oxide, obtained from eq 2a by using the *A* and *B* values reported for s,p-metal and an EN value of $\chi_{Mg} = 1.3$, is in very good agreement with the value of 7.80 eV reported in the literature for single-crystal MgO in a rock-salt structure (rs-MgO) having octahedral coordination.[11] On the other hand, for the two ternary oxides $(Mg)^T[Al_2]^{Oct}O_4$ and $(Mg)^T[Ga_2]^{Oct}O_4$, in the normal spinel structure, the $Mg^{2+}$ species are tetrahedrally coordinated to


https://doi.org/10.1021/acsorginorgau.3c00030
ACS Org. Inorg. Au 2024, 4, 120−134

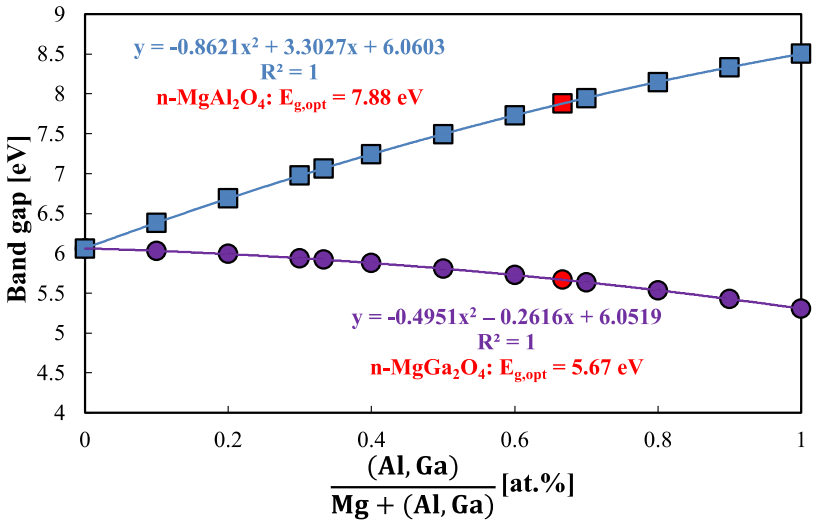


**Figure 1.** Modeling of the optical band gap of ternary oxides $n$-$Mg_{(1-x)}Al_{2x}O_{(1+2x)}$ (squares) and $n$-$Mg_{(1-x)}Ga_{2x}O_{(1+2x)}$ (circles) as a function of Al or Ga content to estimate the $E_{g,opt.}$ values of normal spinels $n$-$MgAl_2O_4$ ($n$-MAO) and $n$-$MgGa_2O_4$ ($n$-MGO) by assuming as binary oxides wz-MgO (see text) and $\alpha$-$Al_2O_3$ for $n$-MAO and wz-MgO and $\alpha$-$Ga_2O_3$ for $n$-MGO. Theoretical band-gap values derived according to eqs 4a−4d by assuming: $A_{wz\text{-}MgO} = 1.6756$, $B_{wz\text{-}MgO} = -2.05$ eV, $\chi_{Mg} = 1.3$, $A_{\alpha-Al_2O_3} = 2.8025$, $B_{\alpha-Al_2O_3} = -2.71$ eV, $\chi_{Al} = 1.5$, $A_{\alpha-Ga_2O_3} = 2.22$, $B_{\alpha-Ga_2O_3} = -2.71$ eV, and $\chi_{Ga} = 1.6$. Continuous lines: fitting lines.

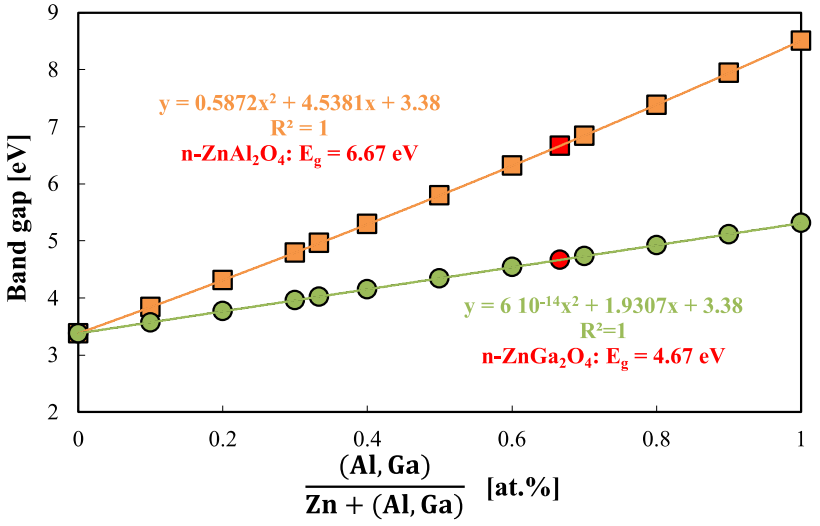


**Figure 2.** Modeling of the optical band gap of ternary oxides $n$-$Zn_{(1-x)}Al_{2x}O_{(1+2x)}$ (squares) and $n$-$Zn_{(1-x)}Ga_{2x}O_{(1+2x)}$ (circles) as a function of Al or Ga content to estimate the $E_{g,opt}$ values of normal spinels $n$-$ZnAl_2O_4$ ($n$-ZAO) and $n$-$ZnGa_2O_4$ ($n$-ZGO) by assuming as binary oxides wz-ZnO and $\alpha$-$Al_2O_3$ for $n$-MAO and wz-ZnO and $\alpha$-$Ga_2O_3$ for $n$-MGO. Theoretical band-gap values derived according to eqs 4a−4d by assuming: $A_{wz\text{-}MgO} = 1.6756$, $B_{wz\text{-}MgO} = -2.05$ eV, $\chi_{Mg} = 1.3$, $A_{\alpha-Al_2O_3} = 2.8025$, $B_{\alpha-Al_2O_3} = -2.71$ eV, $\chi_{Al} = 1.5$, $A_{\alpha-Ga_2O_3} = 2.22$, $B_{\alpha-Ga_2O_3} = -2.71$ eV, and $\chi_{Ga} = 1.6$. Continuous lines: fitting lines.

oxygen ions as in wurtzite phase (wz-MgO), so that we need to derive the $A$ and $B$ values for this s,p-metal oxide in the wurtzite structure. At this aim, we will make use of the results described in previous works[10,12] to derive the two parameters to be used in eqs 3a−3c for calculating the optical band gap of both $n$-spinels. In ref 10, we have shown, starting from eq 1, that it is possible to obtain the following relationship between the $B$ terms for different polymorphs of an oxide $MO_y$

$$B^{wz} = B^{rs} + R_{(MO_y)}/y[1 - (V_{fu}{}^{rs}/V_{fu}{}^{wz})^{2/3}] \quad (5)$$

where $B_{wz}$, $V_{fu}{}^{wz}$, $B_{rs}$, and $V_{fu}{}^{rs}$ represent, respectively, the $B$ parameter and the unit formula volume of the wtz-phase and rs-phase, respectively, while $R_{(MO_y)}$ is the repulsive energy term (see eq 1) of the oxide calculated from the literature data. By assuming for rs-MgO the $B$ value (−2.71 eV) typical of s,p-metal oxides, we will derive the $B$ value for wurtzite MgO according to eq 5 once the unit formula volume of the two polymorphs and the repulsive energy term, $R_{MO_y}$, are known. As for the $A_{wz}$ parameter, it will be derived by using eq 1 and the $E_{g(wz\text{-}MgO)}$ value of 6.06 eV obtained from the fitting of band-gap values as a function of the composition of ternary oxide wz-$(Zn_{(1-x)}Mg_x)O$ ($0 < x_{Mg} < 0.5$) and by extrapolating to $x = 1$.[12] By assuming the experimental value of $V_{fu} = 18.70$ Å$^3$ for the formula unit volume of rs-MgO[17−19] and an average value of $V_{fu} = 23.01$ Å$^3$ for the formula unit volume of wz-MgO, we derive from eq 4a, by using a value of $R_{(MO_y)}/y = 5$ eV, the value of $B_{wz\text{-}MgO} = -2.05$ eV for the wurtzite polymorph of MgO. The term $R_{(MO_y)}/y$ has been


https://doi.org/10.1021/acsorginorgau.3c00030
ACS Org. Inorg. Au 2024, 4, 120−134

obtained by using the lattice energy value of 3795 kJ/mol and a Madelung energy of 4278 kJ/mol.[20] According to this, by using Pauling's EN value of $\chi_{Mg}$ = 1.3 and the band-gap value of 6.06 eV reported above, a value of $A$ = 1.6756 is finally obtained for wz-MgO by means of eq 1 (also see Table S1).

### 1.2. Modeling of the Optical Band Gap of Normal Spinels: *n*-($MgAl_2O_4$, $ZnAl_2O_4$, $MgGa_2O_4$, $ZnGa_2O_4$)

In Figure 1 we report the optical band-gap values of the mixed ternary oxides wtz-MgO//$\alpha$-$Al_2O_3$ and wtz-MgO//$\alpha$-$Ga_2O_3$ as a function of the (Al)/(Al + Mg) and (Ga)/(Ga + Mg) atomic fractions from which it is possible to derive, for $x$ = 0.666, the optical band-gap values of $E_{g,opt}$ = 7.88 eV and $E_{g,opt}$ = 5.67 eV, respectively, for $n$-$MgAl_2O_4$ and $n$-$MgGa_2O_4$ in a normal spinel structure.

The theoretical data have been obtained by means of eqs 4a−4d by using, as $E_{g2}$, the band-gap value of 6.06 eV[21] for wz-MgO, with $A_2$ = 1.6756 and $B_2$ = −2.05 eV, as obtained above, together with an EN value of $\chi_{Mg}$ = 1.3. As for $A_1$ and $B_1$, we used the values reported above for $\alpha$-$Al_2O_3$ together with Pauling's value of EN ($\chi_{Al}$ = 1.5) of aluminum for $n$-$Mg_{(1-x)}Al_xO_{(1+0.5x)}$ data. Relating to $n$-$Mg_{(1-x)}Ga_{2x}O_{(1+2x)}$ data, corresponding parameters of $A$ and $B$ reported for $\alpha$-$Ga_2O_3$ were used[10] together with Pauling's EN value $\chi_{Ga}$ = 1.6 (also see Table S1).

In Figure 2, we report the optical band-gap values of the mixed ternary oxides wtz-ZnO//$\alpha$-$Al_2O_3$ and wtz-ZnO//$\alpha$-$Ga_2O_3$ as a function of the (Al)/(Al + Zn) and (Ga)/(Ga + Zn) atomic fractions from which, for $x$ = 0.666, the optical band-gap values of $E_{g,opt}$ = 6.67 eV and $E_{g,opt}$ = 4.67 eV for $n$-$ZnAl_2O_4$ and $n$-$ZnGa_2O_4$, respectively, in a normal spinel structure were obtained.

The theoretical data have been obtained by means of eqs 4a−4d by using, as $E_{g2}$, the band-gap value (3.37 eV) of wz-ZnO and as $A_2$ and $B_2$ the values typical of d-metal oxide, reported above, together with Pauling's scale EN value of $\chi_{Zn}$ = 1.6. A summary of the modeling parameters used in eqs 4a−4d and of the optical band-gap values estimated for the four $n$-spinels investigated are reported in Tables S1 and 1, respectively.

According to the literature data, an experimental band-gap value of 7.80 eV for a normal $n$-$MgAl_2O_4$ synthetic crystal[6] has been obtained from reflectivity measurements at room temperature, while in more recent works,[7] a band-gap value of around 8.20 eV for ceramic samples[7] and 8.10 eV for a single-crystal sample[25] at 80 and 6 K degrees, respectively, have been reported from photoluminescence investigations. These last values, after correction for the difference of temperature, become at RT equal to 8.03 and 7.87 eV, respectively, for ceramic and single-crystal $n$-MAGO, having assumed a negative coefficient of temperature of about −0.8 meV/K.[6] Both these values are in good agreement with the value of 7.88 eV estimated for $n$-$MgAl_2O_4$ according to our semiempirical approach (see also Table 1). Small differences in the reported $E_g$ values could be traced to the different techniques employed in deriving the band-gap values as well as to the exact structure and composition of the investigated materials.

As for the optical band-gap value, $E_{exp}{}^{opt}$, of $n$-$ZnAl_2O_4$, the experimental data reported in the older literature[3−5] covers a rather large range of values (3.80−5.15 eV), all remaining appreciably smaller with respect to the value (6.67 eV) derived from Figure 2. As evidenced in recent works,[8,22−24] such low band-gap values are noncompatible with the cathodoluminescence data, postulating a much larger fundamental gap, as well as with the measured optical band-gap value, $E_{g,opt.}$ = 6.05 eV, of undoped $ZnAl_2O_4$ samples obtained by hot pressing of powders at the highest temperature (50 MPa, 1600 °C) and in the presence of a sintering additive ($ZnF_2$).[25]

According to this, the lower optical band-gap values reported in the literature could be related

(a) To the presence of specific defects in the crystalline structure of the investigated materials[55] originating bands of donor and acceptor electronic states within the forbidden gap of the $n$-$ZnAl_2O_4$ spinel.

(b) To the coexistence of a Zn-rich mixed $ZnO/Al_2O_3$ oxide phase, originated during the fabrication process of samples, having lower optical band values.

This last hypothesis is compatible with the X-rays data analysis at different temperatures, reported in ref 8, and showing how at a temperature of 1000 °C, the formation of a $ZnAl_2O_4$ spinel is compatible with the presence of ZnO and $\gamma$-$Al_2O_3$ phases.

However, we have to point out, see Table 1, that the direct optical band-gap value (6.05 eV) of the $n$-ZAO ceramic sample, with an average grain size of about 33 $\mu$m, as reported in ref 24, is still 0.62 eV lower than the theoretical value (6.67 eV) estimated by us and 0.9 eV lower than the average exciton energy peak, $E^{exc}$ = 6.95 ± 0.1 eV, of $ZnAl_2O_4$ powders and nanofibers.[8,22−24] A possible explanation for the difference between the $E_g$ values reported in Table 1 could be traced to the fact that in the presence of an excitonic gap, the fundamental energy gap is lowered by the electron−hole binding energy of the first exciton near the fundamental gap. We have shown, in very recent work on aluminum garnets,[10] that in these cases, it is possible to derive, between the optical band gap (or optical energy absorption onset) $E_{g,opt}$ and the first exciton energy peak $E^{exc}$, the following relationship

$$E^{exc} = (E_{g,opt} + 0.25) \pm 0.1 \text{ eV} \quad (6)$$

In order to get the fundamental energy gap, $E_{g,f}$, we need to add to $E^{exc}$ the electron−hole binding energy of the exciton.[10] As suggested by Dorenbos,[56−58] for aluminum garnets, we can get a good estimate of the fundamental energy gap by using, as a first approximation, $E^{exc}$ and the relationship

$$E_{g,f} = E^{exc}(1 + 0.008E^{exc})\text{eV} \quad (7)$$

We have to say that the realm of validity of eq 7 encompasses a class of materials wider than the aluminum garnets, while eq 6 needs to be tested outside the range of materials investigated in ref 9. For these reasons, when the $E^{exc}$ term was accessible, we derived the $E_{g,f}$ value reported in Table 1 by means of eq 7, while, in the absence of such information, we used eqs 6 and 7 if the $E_{g,opt}$ value was known.

As for the $MgAl_2O_4$ crystal for which an inversion degree ($i$ = 0.12) has been very recently reported,[26] the fundamental gap $E_f$ = 7.88 eV (see Table 1), derived by using eq 7 and the experimental value of $E^{exc}$ = 7.434 eV derived from ref 26., after correction for the difference of temperature is also in good agreement with the theoretical values ($E^{th}$ = 7.88−7.80 eV) derived by using our semiempirical approach or the DFT-based hybrid-TB-mBJ model[29,31,32] (Tran−Blaha-modified Becke−Johnson potential) for treating the local exchange−correlation energy. The small difference in energy (0.2−0.3 eV) between the experimental fundamental gap, $E_f$, and $E_g{}^{th}$ value could be traced to the presence of a small inversion degree owing to a partial occupancy of octahedral sites by $Mg^{2+}$ cations. Inversion degrees


https://doi.org/10.1021/acsorginorgau.3c00030
ACS Org. Inorg. Au 2024, 4, 120−134

between 0.12 and 0.38 ($0.12 < i < 0.40$) have been reported in the literature for $MgAl_2O_4$ crystalline samples.[26,59,60]

In the case of $ZnAl_2O_4$ powder samples, by using eq 7 and the $E^{exc}$ values reported in Table 1, we obtained $E_f$ values ($E_f = 7.28 \pm 0.1$ eV) much higher than the experimental older $E_{g,opt}$ values (3.80−5.15 eV) but near to the value estimated by our approach (6.67 eV) or by DFT-based calculations.[33,34,52] In the case of ceramic samples,[25] with an average grain size of 33 $\mu$m, grown by hot pressing (50 MPa) at a very high temperature (1600 °C), a value of $E_f = 6.62$ eV was obtained by using eqs 6−7 and the reported direct optical band gap of 6.05 eV[25] in very good agreement also with our estimated value (6.67 eV).

We have to say that the theoretical band-gap values, estimated by us or derived from DFT-based methods, pertain to bulk crystalline materials, where quantum size effects are absent. In the presence of powdered samples, with grain size in the order of a few nanometers, both $E_{g,opt}$ and $E^{exc}$ values can be modified by the possible presence of quantum size effects. According to this, a band-gap dependence from the average grain size has been reported as[49]

$$\Delta E_g(\text{eV}) = E_g(D) - E_{g,b} = K/D^n$$

where $E_g(D)$ is the band gap of the material with average grain dimension $D$, $E_{g,b}$ is the band gap of the bulk semiconductor, and $K$ and $n$ are two constants depending on the material preparation and thickness dimensional unity, respectively. For ZnO samples, with $D$ in nm, $K = 3.23$, and $n = 1.65$, an increase of $E_g$ in the order of about 0.23 eV has been reported for ZnO particles having average grain size in the order of 5 nm. Analogous dependence from grain thickness, but with $K = 926$ and $n = 1.62$, has been reported for the increase of the first exciton binding energy, $\Delta E^{ex}$(meV), which for undoped ZnO samples of average grain size $D = 5$ nm should amount to 68.3 meV.[49] Owing to the small binding energy of the exciton in ZnO, the largest contribution to the increase of band-gap energy, $\Delta E_g \sim 0.3$ eV, of zinc oxide nanoparticles comes out from the increase in the optical gap value.

In the case of $ZnAl_2O_4$ powder samples, a wide range of average particle sizes ($4 < D_{av} < 24$ nm) has been reported in the literature depending both on the synthesis process and after-synthesis treatments employed by different research groups.[38,61,62] It is worth noting that for $ZnAl_2O_4$ particles, variations in the optical gap values comprised between 0.55 eV, for particle size of about 20 nm, and 0.76 eV, for particle size in the order of 12 nm, have been reported with respect to larger particle sizes of about 24 nm.[62] Apart from the small differences in the reported $\Delta E_g(D)$ values, probably depending on possible differences in composition and crystalline defects present in the different samples synthesized by different routes, we like to stress that the average $\Delta E_{g,av}(D)$ value is equal to $0.65 \pm 0.1$ eV. This average $\Delta E_{g,av}(D)$ value is in very good agreement with the energy difference between experimentally derived $E_f$ values and reported in Table 1 for bulk ($E_f = 6.62$ eV) or powders (7.28 eV) $ZnAl_2O_4$ samples. We stress that the band-gap value estimated by us (6.67 eV in Table 1) is in very good agreement with all of the experimental $E_f$ values obtained after correction for grain dimensions of ZAO powders samples. Owing to a much lower inversion degree ($0 < i < 0.063$) reported[8] for $ZnAl_2O_4$, no further appreciable corrections to the reported band-gap values should be expected for $ZnAl_2O_4$ samples.

From Figures 1 and 2, the optical band-gap values of 5.67 and 4.67 eV were derived, respectively, for $MgGa_2O_4$ ($n$-MGO) and $ZnGa_2O_4$ ($n$-ZGO) normal spinels by using the $A$ and $B$ parameters and values of $E_{g2}$ reported above for wz-MgO and wz-ZnO. Analogously to the corresponding aluminates we used in eqs 4a−4d, the values of $A$ (2.22) and $B$ (−2.71 eV) previously reported for $\alpha$-$Ga_2O_3$ which correspond, according to eq 1, to an $E_{g,opt}$ value of 5.30 eV by assuming for gallium metal an EN value $\chi_{Ga} = 1.60$ in Pauling's scale.[14] As expected, according to eq 1, lower optical band-gap values are obtained for gallates with respect to aluminates as well as for zinc-containing spinels with respect to those containing magnesium. Such an expected trend is also in agreement with the trend observed in band-gap values calculated by using different DFT-based models.[33]

For $n$-MGO samples, fewer experimental optical band-gap values have been reported in the literature, but two recent papers[37,63] report direct optical band-gap values of 5.03 eV for a partially inverse MGO single crystal[37] and of 5.15 eV for an MOCVD film[63] for which the inversion degree was not reported. Older data, pertaining to the electroluminescence properties of MGO samples, provide information on the presence of an exciton energy peak at around 5.25 eV,[39] without any mention of the possible inversion degree, while in the case of a sample,[40] with a partial inversion degree of $i = 0.44$, an exciton energy peak of about 5.36 eV is reported. We stress that both experimental $E^{exc}$ values are lower than the value of the band gap (5.67 eV) derived for the $n$-$MgGa_2O_4$ sample (see Figure 1). By using eq 6 and the optical band-gap values (5.03−5.15 eV) reported above for MGO, we get a value of $E^{exc}$ (5.28−5.40) $\pm$ 0.1 eV in very good agreement with the value of 5.41 $\pm$ 0.05 eV reported in Table 1. By using eq 7 and the value of $E^{exc} = 5.40$ eV, we obtain a fundamental gap equal to 5.63 eV, while from the experimental $E_g^{opt}$ data, reported above, we obtain for MGO a value of $E_f = 5.57 \pm 0.1$ eV. Both $E_f$ values, derived from different experimental data and techniques, are in good agreement with the value (5.67 eV) calculated by means of eqs 4a−4d, lending further support to the suggested approach. We have to mention that the MGO spinel, in the ground state, has been reported[30] as an inverse spinel ($i = 1$), while lower inversion degree values ($0.40 < i < 0.88$) have been experimentally measured.[40,63] From the data of Table 1, it comes out that, regardless of the inversion degree, the experimentally estimated $E_f$ data agree nicely with the band-gap value of $n$-MGO calculated in Figure 1 by our semiempirical approach. The DFT-based value ($E_f = 2.63$ eV) calculated[29] by using the generalized gradient approximation (GGA-PBE-modified) greatly differs from the above-reported $E_f$ values as well as from experimental optical band-gap values. The absence of any appreciable dependence of $E_f$ values from the inversion degree is an interesting finding that will be fully rationalized after deriving the band-gap value of the corresponding inverted spinel (see Section 2).

As for $n$-ZGO, a range of optical band-gap values have been reported in the literature with the lower values ($E^i_{g,opt} \sim 4.60 \pm 0.05$ eV),[42,43] usually, attributed to the presence of an indirect optical gap and the highest ones ($E_{g,opt}{}^d \sim 4.80 \pm 0.10$ eV) to a direct gap.[23,48,49,55,56,64,65] On the other hand, for ZGO powder samples, grown via a solid-state route at high temperatures (1200−1400 °C), from photoluminescence excitation spectra an exciton peak energy at 245 nm ($E^{exc} = 5.05$ eV) was measured[66] from which a fundamental energy gap $E_f = 5.25$ eV was derived by means of eq 7. The value of $E^{exc}$ is in good agreement with the direct optical band-gap values as well as with other $E^{exc}$ values reported in Table 1. As for the $E^{exc}$ values of Table 1, we like to stress that for the ZGO sample prepared via a similar synthetic route, a slightly lower exciton energy peak ($E^{exc}$


https://doi.org/10.1021/acsorginorgau.3c00030
ACS Org. Inorg. Au 2024, 4, 120−134

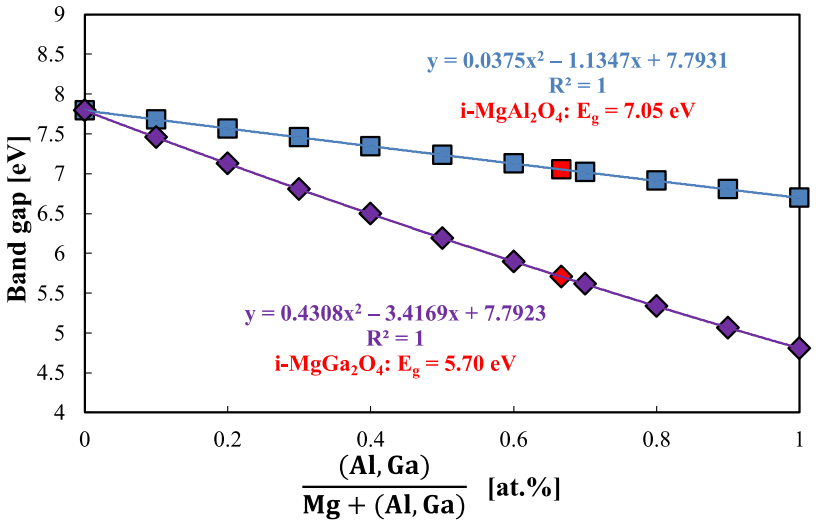


**Figure 3.** Modeling of the optical band gap of ternary oxides *i*-$Mg_{(1-x)}Al_{2x}O_{(1+2x)}$ (squares) and *i*-$Mg_xGa_{(1-x)}O_{(1.5-x)}$ (diamonds) as a function of Al or Ga content to estimate the $E_{g,opt.}$ values of inverted spinels *i*-$MgAl_2O_4$ (*i*-MAO) and *i*-$MgGa_2O_4$ (*i*-MGO) by assuming as binary oxides rs-MgO and *β*-$Al_2O_3$ for *i*-MAO and rs-MgO and *β*-$Ga_2O_3$ for *i*-MGO. Theoretical band-gap values derived according to eqs 4a−4d by assuming: $A_{rs\text{-}MgO} = 2.17$, $B_{rs\text{-}MgO} = -2.71$ eV, $\chi_{Mg} = 1.3$, $A_{\beta-Al_2O_3} = 2.2313$, $B_{\beta-Al_2O_3} = -2.225$ eV, $\chi_{Al} = 1.5$, $A_{\beta-Ga_2O_3} = 1.9695$, $B_{\beta-Ga_2O_3} = -2.31$ eV, and $\chi_{Ga} = 1.6$.

= 4.95 eV) has been reported[40] in presence of a mentioned partial inversion degree of the ZGO spinel. More recently, for *n*-ZGO films grown by the MOCVD technique,[67] a band-gap value of 5.25 eV has been reported on the basis of a detailed cathodoluminescence study. Moreover, this band-gap value agrees nicely with the direct band-gap value (5.27 eV) of the ZGO single crystal obtained by Hilfiker et al.[53] by spectroscopic ellipsometry analysis. From this detailed analysis of different techniques employed, it seems reasonable to assume a value of 5.2 ± 0.05 eV for the fundamental energy gap of *n*-$ZnGa_2O_4$ from which an average optical band-gap value of 4.75 eV can be derived by means of eqs 6 and 7. This average $E_{g,opt}$ value is also in good agreement with the band-gap value of 4.67 eV derived in Figure 2 by using our semiempirical approach (also see Table 1).

By summarizing the results reported in Table 1, we can say that our semiempirical approach is able to provide the fundamental band-gap values for cubic normal spinel oxides investigated, with a partial exception for $ZnGa_2O_4$ samples for which a good agreement is observed with the range of optical band-gap values reported in the literature.

## 2. BAND-GAP MODELING OF INVERTED SPINELS *I*-(MAO, ZAO, MGO, ZGO)

From the general chemical formula written as $(A_{1-i}B_i)^T[A_iB_{2-i}]^{Oct}O_4$, where *i* represents the inversion degree for partially ($i < 1$) inverted spinels, we can derive the following structures for totally ($i = 1$) inverted spinels: $(B_1)^T[A_1B_1]^{Oct}O_4$, where B = Al,Ga and A = Mg,Zn. According to the chemical formula, for $i = 1$, in the inverted spinels, both $Zn^{2+}$ and $Mg^{2+}$ ions will occupy only octahedral voids, typical of MgO and ZnO polymorphs in the rock-salt structure. On the other hand, only 50% of $Al^{3+}$ and $Ga^{3+}$ ions will occupy octahedral voids, while the remaining 50% are located in tetrahedral voids typical of the wurtzite structure. In order to use eqs 3a−3c, we need to identify which of the numerous gallia and alumina polymorphs is compatible with ternary oxides having a totally inverted spinel structure. As reported in the literature,[16] the structure of *θ*-alumina (currently identified as *β*-$Al_2O_3$) is the only polymorph where 50% of $Al^{3+}$ ions occupy tetrahedral sites, while the other remaining 50% occupy octahedral sites. According to this, the modeling of the optical band gap of ternary oxides *i*-$(Al)^T[MgAl]^{Oct}O_4$ and *i*-$(Al)^T[ZnAl]^{Oct}O_4$ will be carried out by using in eqs 4a−4d, as binary oxides, the rs-polymorphs for MgO and ZnO oxides and the *β*-$Al_2O_3$ phase for alumina. By analogy, in the case of gallate spinels, we will assume the *β*-$Ga_2O_3$ polymorph as a partner of rs-MgO and rs-ZnO in mixed ternary oxide *i*-$MgGa_2O_4$ and *i*-$ZnGa_2O_4$ inverted spinels. As for the *β*-gallia and *β*-alumina polymorphs, we will use the *A* and *B* values previously derived and reported in Tables 1−2 of ref 2., while for rs-MgO, we will employ the *A* and *B* values typical of s,p-metal oxides ($A = 2.17$, $B = -2.71$ eV) (see Table S1).

In the case of rs-ZnO, we derived the *A* and *B* parameters by following the same procedure, as described above, to obtain the *A* and *B* parameters of wz-MgO. To derive the *B* value of rs-ZnO, by means of eq 5, we used for the two ZnO polymorphs[68] the formula unit volume values of $V_{fu}(rs) = 19.48$ Å$^3$ and $V_{fu}(wz) = 23.75$ Å$^3$, for rs-ZnO and wz-ZnO, respectively, with a value of 5.5 eV for the repulsive energy term $R_{(MO_y)}/y$. This last value has been obtained by using an average lattice energy[20] $U_L = 4056$ kJ/mol and a Madelung energy[69] $U_M = 4586$ kJ/mol. After substitution in eq 5, the *B* value of −2.18 eV is obtained for rs-ZnO. To obtain the parameter *A*, we used in eq 1 the band-gap value of 2.80 eV for rs-ZnO, derived[21] from the fitting of the band-gap values of ternary rs-$(Mg_{(1-x)}Zn_x)O$ as a function of Zn content in the alloy ($0 < x_{Zn} < 0.5$) and by extrapolating $x_{Zn}$ to 1, together with the value of $B = -2.18$ eV reported above. After substitution of $E_g$ (2.80 eV) and *B* (−2.18 eV) in eq 1, a value of $A_{(rs\text{-}ZnO)} = 1.38$ is obtained according to the relationship: $A_{rs} = (E_{g,opt} + B_{rs})/(\chi_O - \chi_{Zn})^2$ and by using the EN values, in Pauling's scale, of 3.5 for oxygen and 1.60 for zinc.

From the data of Figure 3, pertaining to the modeling of the optical band gap of ternary oxides rs-MgO//*β*-$Al_2O_3$ (squares) and rs-MgO//*β*-$Ga_2O_3$ (diamonds), we obtain, for $x = 0.666$, the optical band-gap values of 7.05 and 5.70 eV for *i*-$MgAl_2O_4$ and *i*-$MgGa_2O_4$, respectively.

We are not aware of experimental data of $E_{g,opt}$ as a function of the inversion degree for *i*-$MgAl_2O_4$, but in a recent theoretical study on magnesium−aluminate[64] by Pathak et al., the authors


https://doi.org/10.1021/acsorginorgau.3c00030
ACS Org. Inorg. Au 2024, 4, 120−134

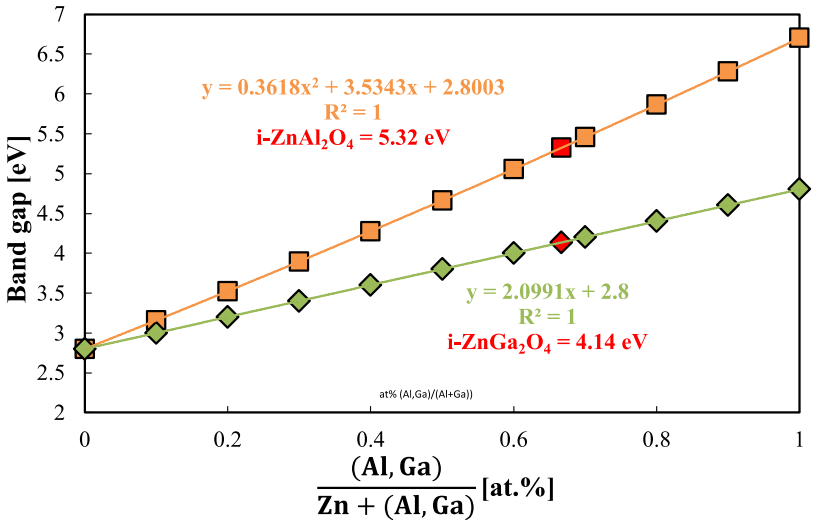


**Figure 4.** Modeling of the optical band gap of ternary oxides $i$-$Zn_{(1-x)}Al_{2x}O_{(1+2x)}$ (squares) and $i$-$Zn_{(1-x)}Ga_{2x}O_{(1+2x)}$ (diamonds) as a function of Al or Ga content to estimate the $E_{g,opt}$ values of inverted spinels $i$-$ZnAl_2O_4$ ($i$-ZAO) and $i$-$ZnGa_2O_4$ ($i$-ZGO) by assuming as binary oxides rs-ZnO and $\beta$-$Al_2O_3$ for $i$-ZAO and rs-ZnO and $\beta$-$Ga_2O_3$ for $i$-MGO. Theoretical band-gap values were derived according to eqs 4a−4d by assuming: $A_{rs\text{-}ZnO} = 1.38$, $B_{rs\text{-}ZnO} = -2.18$ eV, $\chi_{Zn} = 1.6$, $A_{\beta-Al_2O_3} = 2.2313$, $B_{\alpha-Al_2O_3} = -2.225$ eV, $\chi_{Al} = 1.5$, $A_{\beta-Ga_2O_3} = 1.9695$, $B_{\alpha-Ga_2O_3} = -2.31$ eV, and $\chi_{Ga} = 1.6$.

estimated a decrease of 1.05 eV in the band gap of $i$-$MgAl_2O_4$ with respect to $n$-$MgAl_2O_4$. By assuming the band gap of $n$-$MgAl_2O_4$ as near 8 eV (see above), the value of $E_g = 7.05$ eV, obtained in Figure 3, for the inverted $MgAl_2O_4$ ($i = 1$) spinel is in quite good agreement with the estimated decrease reported in the literature.[64]

Further support in favor of the estimated $E_g$ value (7.05 eV) for $i$-MAO is obtained by a careful inspection of the experimental data reported in Table 1 for the $MgAl_2O_4$ crystal for which an inversion degree $i = 0.12$ has been reported in a very recent work.[27] By using a linear connection formula, as a function of the inversion parameter, and the value of $E_g$ reported by us for the $i$-$MgAl_2O_4$ sample and the $E_f$ of Table 1 for the partially ($i = 0.12$) inverted MAO, we can write for the partially ($i = 0.12$) inverted spinel

$$E_{f,(i=0.12)} = 0.12 \times 7.05 + 0.88 \times E_f(n\text{-MAO}) = 7.88 \text{ eV}$$

By solving the previous equation for $n$-MAO, a value of 7.99 eV is obtained for $n$-$MgAl_2O_4$ ($i = 0$) spinel oxide, in very excellent agreement with the experimental band-gap value of 8.0 eV suggested for $n$-MAO[7,26,27] and in good agreement with the band-gap value obtained by our semiempirical approach.

In the case of gallate, we like to stress that the band-gap values of $n$-$MgGa_2O_4$ (5.67 eV) and $i$-$MgGa_2O_4$ (5.71 eV) spinels are almost equal and in good agreement with the band-gap value of a partially inverted $i$-MGO sample ($i = 0.44$) showing an exciton energy peak value $E^{exc} = 5.40$ eV[39,40] from which a fundamental band-gap value $E_f = 5.63$ eV is obtained by means of eq 7. At variance with the experimental data, theoretical band-gap values of 5.80−5.11 eV for $n$-$MgAl_2O_4$,[28,30] 5.51 eV for $i$-$MgAl_2O_4$,[28] and 2.63 eV for $i$-$MgGa_2O_4$,[30] respectively, have been estimated by using DFT-based methods.

In Figure 4, we report the behavior of ternary mixed oxides rs-ZnO//$\beta$-$Al_2O_3$ (square symbol) and rs-ZnO//$\beta$-$Ga_2O_3$ (diamonds) as a function of the composition ratios, $x_{Al} = Al/(Zn + Al)$ and $x_{Ga} = Ga/(Zn + Ga)$, from which the values of $E_g$ equal to 5.32 and 4.14 eV are obtained for $i$-$ZnAl_2O_4$ and $i$-$ZnGa_2O_4$, respectively, at $x = 0.666$.

We are not aware of experimental and theoretical data pertaining to the band gaps of both inverted $i$-ZAO and $i$-ZGO spinels ($i = 1$), but different band-gap values for partially inverted $i$-ZAO and $i$-ZGO samples have been reported. From the literature data,[25,39,40,42,46,48,60] it comes out that the inversion degree of the spinel oxides investigated strongly depends on the synthetic procedure and thermal treatments after preparation. However, regardless of the preparation methods, the inversion degree of ZAO ($i \leq 0.05$) is, usually, much lower than that of ZGO ($i \leq 0.3$) or MGO ($i \leq 0.80$) and MAO ($i \leq 0.2$).[59]

In Table 2, we report the band-gap values of inverse ($i = 1$) or partially inverse spinels ($0 < i < 1$) obtained experimentally or theoretically estimated.

As for $ZnGa_2O_4$, values of the inversion parameter equal to $i = 0.30$ and $i = 0.17$ have been reported for samples obtained by different routes.[46] By using the Tauc plot in both cases, a direct optical band-gap value of 4.75 eV was measured for the sample $(Zn_{.70}Ga_{.30})^T(Zn_{.30}Ga_{1.70})^{Oct.}O_4$ prepared by the precursor route ($i = 0.30$), whereas for the sample $(Zn_{.83}Ga_{.17})^T(Zn_{.17}Ga_{1.83})^{Oct.}O_4$ obtained by a solid-state method ($i = 0.17$), a value of 4.53 eV was measured for $E_{g,opt.}$ In both cases, the $E_{g,opt.}$ values are in the range of values reported in the literature for the ZGO spinel, but we like to stress that for the sample prepared via the solid-state method, the agreement between measured (4.53 eV) and calculated (4.51 eV) $E_{g,opt.}$ values is better than for the sample prepared by the precursor route ($\Delta E_{g,opt.} = 0.17$ eV).

The larger $\Delta E_{g,opt.}$ term for the precursor route sample is in agreement with the hypothesis of quantum size effects, as discussed above, owing to the large difference in crystallite sizes reported[46] for these samples with respect to the sample prepared via the solid-state route.

In Table 2, we reported the estimated band-gap values of inverted spinels with $i \leq 1$ for which the experimental band gap, $E_{g,opt.}$ or $E_f$, and the inversion degree, $i$, values have been reported in the literature.

It is worth noting the good agreement between the reported[39,40] band-gap value $E_g = 5.63$ eV of $MgGa_2O_4$, at $i = 0.44$, and that estimated by our semiempirical approach ($E_g =$


https://doi.org/10.1021/acsorginorgau.3c00030
ACS Org. Inorg. Au 2024, 4, 120−134

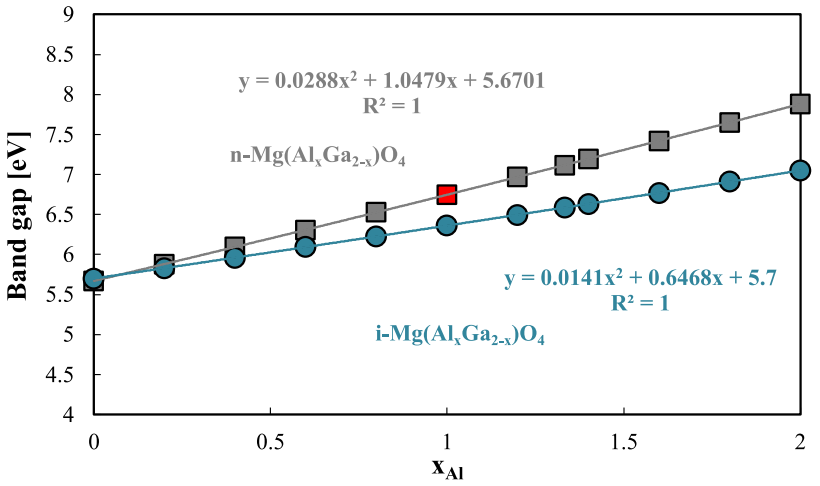


**Figure 5.** Modeling of optical band-gap values of doubles spinel $Mg(Al_xGa_{(1-x)})_2O_4$ (MAGO) as a function of Al composition for ($i = 0$) *n*-MAGO (squares) and for ($i = 1$) *i*-MAGO (circles). Theoretical band-gap values have been derived by using eqs 9 and 9a−9d with $E_{gT2} = 5.67$ eV, $A_{2av} = 2.038$, $B_{2av} = -2.49$ eV, $\chi_{2av} = 1.50$, $A_{1av} = 2.427$, $B_{1av} = -2.49$ eV, and $\chi_{1av} = 1.433$ for *n*-MAGO and with $E_{gT2} = 5.70$ eV, $A_{2av} = 2.036$, $B_{2av} = -2.443$ eV, $\chi_{2av} = 1.50$, $A_{1av} = 2.211$, $B_{1av} = -2.387$ eV, and $\chi_{1av} = 1.433$ for *i*-MAGO.

5.68 eV) at variance with the much lower $E_g$ value (2.63 eV) of *i*-MGO, estimated by DFT-based methods.[30]

## 3. BAND-GAP MODELING OF DOUBLE SPINELS (Mg, Zn)$(Al_xGa_{2-x})O_4$

By using the results of our recent study[9] on quaternary oxides as well as those reported above for the different polymorphs of ZnO and MgO, we will apply our semiempirical approach to the modeling of the following quaternary systems: (wz-ZnO, wz-MgO)//$(\alpha$-$Al_xGa_{2-x})O_3$ and (rs-ZnO, rs-MgO)//$(\beta$-$Al_xGa_{2-x})$. With respect to the single spinel, for which we wrote the general formula $(A_{1-i}B_i)^T[A_iB_{2-i}]^{Oct.}O_4$, where only two different cations *A* (usually representing the bivalent cation, $Mg^{2+}$ or $Zn^{2+}$) and *B* (usually indicating a trivalent cation, $Al^{3+}$ or $Ga^{3+}$) are present in different concentrations, on tetrahedral (T) and octahedral (Oct) sites, in the case of double spinels we are, generally, in the presence of three different cations so that, by following Ito et al.,[59] we can write the following general formula

$$(A_{1-i}B^1_jB^2_{(i-j)})^T[A_iB^1_{(2-x-j)}B^2_{(x-i+j)}]^{oct.}O_4 \quad (8)$$

where

(a) *A* is the bivalent cation ($Mg^{2+}$ or $Zn^{2+}$) and $B^1$ and $B^2$ represent the trivalent cations, in our case, respectively, $Al^{3+}$ and $Ga^{3+}$.

(b) *j* is the occupancy for $B^1$ in the 4-fold (or tetrahedral) coordinated site and *i* is the occupancy for $A^{+2}$ in the 6-fold (or octahedral) coordinate site (or inversion parameter).

In the case of the Mg double spinel, eq 8 becomes

$$(Mg_{1-i-j}Al_jGa_{i-j})^T[Mg_iAl_{2-x-j}Ga_{x-i+j}]^{oct.}O_4 \quad (8a)$$

which for the *n*-double spinel ($i = 0$, $j = 0$) can be rewritten as

$$(Mg_1)^T[Al_{2-x}Ga_x]^{oct.}O_4 \quad (8b)$$

while for the Zn *n*-double spinel, it becomes

$$(Zn_1)^T[Al_{2-x}Ga_x]^{oct.}O_4 \quad (8c)$$

Equations 8b and 8c, with $0 \le x \le 2$, represent two quaternary oxide systems as a function of the composition variable where the end terms (for $x = 0$ and $x = 2$) coincide with ternary systems representing the normal spinels: $MgAl_2O_4$, $MgGa_2O_4$, $ZnAl_2O_4$ and $ZnGa_2O_4$. These findings agree with our previous results pertaining to the quaternary alumina garnet phases.[10]

By analogy with our previous treatment of quaternary alumina garnets,[10] we will model the optical band gap of these double spinels by means of eqs

$$E_{g,q}(\chi_{av}) = E_{g,T2} + S_l(q)x_l + S_q(q)x_l^2 + S_c(q)x_l^3$$
$$\text{with: } 0 \le x_{Al} \le 1 \quad (9)$$

where

$$E_{g,T2} = A_{2,av(T_2)}(\chi_O - \chi_{2,av})^2 + B_{2,av(T_2)} \quad (9a)$$

is the band gap of the ternary systems (*n*-$MgGa_2O_4$ or *n*-$ZnGa_2O_4$) corresponding to aluminum atomic fraction $x_{Al} = 0$ in eq 9. The coefficients of the cubic eq 9 are now written as

$$S_l(q) = 2A_{2T,av}(\chi_O - \chi_{T2,av})(\chi_{T2,av} - \chi_{T1,av}) + (B_{1T,av} - B_{2T,av}) + (A_{1T,av} - A_{2T,av})(\chi_O - \chi_{T2,av})^2 \quad (9b)$$

$$S_q(q) = 2(A_{1T,av} - A_{2T,av})(\chi_O - \chi_{T2,av})(\chi_{T2,av} - \chi_{T1,av}) + A_{2T,av}(\chi_{T1,av} - \chi_{T2,av})^2 \quad (9c)$$

$$S_c(q) = (A_{1T,av} - A_{2T,av})(\chi_{T1,av} - \chi_{T2,av})^2 \quad (9d)$$

The parameters $(A_{1T,av}/A_{2T,av})$ and $(B_{1T,av}/B_{2T,av})$ to be used in eqs 9a−9d are the weighted at% average of $A_i$, $B_i$, and $\chi_i$ parameters of ternary end terms of eq 8a (or 8b) corresponding to the different polymorphs of the two ternary subsystems. In our case, as for *n*-$(Mg_1)^T[Al_{2-x}Ga_x]^{Oct.}O_4$ (*n*-MAGO), for $x = 2$, we will have

$$A_{2,av} = \frac{A_{(wz\text{-}MgO)} + 2A_{(\alpha\text{-}Ga_2O_3)}}{3} \qquad A_{1,av} = \frac{A_{(wz\text{-}MgO)} + 2A_{(\alpha\text{-}Al_2O_3)}}{3}$$

$$\chi_{2,av} = \frac{\chi_{Mg} + 2\chi_{Ga}}{3} \qquad \chi_{1,av} = \frac{\chi_{Mg} + 2\chi_{Al}}{3}$$

$$B_{2,av} = \frac{B_{(wz\text{-}MgO)} + 2B_{(\alpha\text{-}Ga_2O_3)}}{3} \qquad B_{1,av} = \frac{B_{(wz\text{-}MgO)} + 2B_{(\alpha\text{-}Al_2O_3)}}{3}$$



https://doi.org/10.1021/acsorginorgau.3c00030
ACS Org. Inorg. Au 2024, 4, 120−134

Table 3. Band-Gap Values of Double Spinels ($i = 0$, $i = 1$) Estimated by the Semiempirical Approach, $E_g^{th}$, Experimental Optical Gap Values $^{d,i}E_{exp}^{opt}$ Obtained by Tauc's Method (d: Direct; i: Indirect), Experimental Excitation Peak Energy Values of the Excitonic Gap $E_{exp}^{exc}$, Experimental Fundamental Band Gap, $E_f^{exp}$, Obtained (through eqs 6 and 7) from $E_{exp}^{exc}$ or $E_{exp}^{opt}$, and Theoretical $E_f^{th}$ Obtained (through eqs 6 and 7) from $E_g^{th,opt}$

| phase | $E_g^{th}$ [eV] | $E_{exp}^{opt}$ [eV] | $E_{exp}^{exc}$ [eV] | $E_g$ (DFT) [eV] | $E_f^{exp}$ [eV] | $E_f^{th}$ [eV] |
|---|---|---|---|---|---|---|
| *n*-$Mg(AlGa)O_4$ | 6.75 | | | | | |
| *i*-$Mg(AlGa)O_4$ | 6.36 | | | 3.33[30] | | |
| *n*-$Mg(Al_{1.5}Ga_{0.5})O_4$ | 7.30 | | | | | |
| *i*-$Mg(Al_{1.5}Ga_{0.5})O_4$ | 6.70 | | | | | |
| *n*-$Zn(Al_{0.2}Ga_{1.8})O_4$ | 4.85 | | 5.1[51] | | 5.30[51] | 5.30 ± 0.1 |
| *n*-$Zn(Al_{0.5}Ga_{1.5})O_4$ | 5.14 | | 5.22[51] | | 5.44[51] | 5.62 ± 0.1 |
| *n*-$Zn(Al_1Ga_1)O_4$ | 5.63 | | | | | |
| $\gamma$–$Zn(Al_1Ga_1)O_4$ | 4.96 | ($4.53^d$ – $4.58^d$)[71] | | | 4.96–5.01[71] | |

By substituting the corresponding values to $A_i$, $B_i$, and $\chi_i$ parameters, we get for *n*-$MgGa_2O_4$

$$A_{2,av} = (1.6756 \times 1 + 2.22 \times 2)/3 = 2.038$$

$$\chi_{2,av} = (1.3 \times 1 + 1.6 \times 2)/3 = 1.5$$

$$B_{2,av} = -2.49 \text{ eV}$$

while for *n*-$MgAl_2O_4$, we obtain

$$A_{1,av} = (1.6756 \times 1 + 2.8025 \times 2)/3 = 2.427$$

$$\chi_{1,av} = (1.3 \times 1 + 1.5 \times 2)/3 = 1.433$$

$$B_{1,av} = -2.49 \text{ eV}$$

### 3.1. Double Spinels: *n,i*-$Mg(Al_xGa_{2-x})O_4$ or (*n,i*-MAGO)

In Figure 5, we plot the optical band-gap values, for the normal double spinel *n*-MAGO, as a function of the composition variable in all of the ranges of composition, $0 \le x_{Al} \le 2$, embodied in eq 8a.

As mentioned above, the end points ($x = 0$ and $x = 2$) coincide with the band-gap values of ternary spinels *n*-$MgGa_2O_4$ (5.67 eV) and *n*-$MgAl_2O_4$ (7.88 eV), while a value of 6.75 eV is obtained for the double spinel *n*-$Mg(AlGa)O_4$ corresponding to $x = 1$. This last value is an intermediate one between the two end-term values and probably not different from the real one if we take into consideration that some inversion degree can be expected owing to the tendency of $Mg^{2+}$ to substitute the $Ga^{3+}$ species in octahedral coordination. By taking into account that the *i*-$MgGa_2O_4$ spinel has a band gap (5.70 eV) quite similar to *n*-$MgGa_2O_4$, we can conclude that the band gap of the *n*-double spinel should not change too much in presence of a partial inversion. By analogy with the approach followed for the normal double spinel $(Mg_1)^T[Al_xGa_{(2-x)}]^{Oct}O_4$, we plot in Figure 5 the optical band gap of the inverted spinel derived from eq 8 by assuming $i = 1$ and with the initial hypothesis that in the ternary mixed oxide $\beta$-$Al_xGa_{(2-x)}$, the occupancy of tetrahedral and octahedral sites by $Ga^{3+}$ and $Al^{3+}$ in the mixed oxide follows the same trend existing in the pure $\beta$-$Al_2O_3$ and $\beta$-$Ga_2O_3$. According to this initial assumption and by following the same procedure reported above for the quaternary spinel oxides, we used again eqs 9a–9d by using the corresponding parameters

$$A_{2,av} = \frac{A_{(rs\text{-}MgO)} + 2A_{(\beta\text{-}Ga_2O_3)}}{3} \qquad A_{1,av} = \frac{A_{(rs\text{-}MgO)} + 2A_{(\beta\text{-}Al_2O_3)}}{3}$$

$$\chi_{2,av} = \frac{\chi_{Mg} + 2\chi_{Ga}}{3} \qquad \chi_{1,av} = \frac{\chi_{Mg} + 2\chi_{Al}}{3}$$

$$B_{2,av} = \frac{B_{(rs\text{-}MgO)} + 2B_{(\beta\text{-}Ga_2O_3)}}{3} \qquad B_{1,av} = \frac{B_{(rs\text{-}MgO)} + 2B_{(\beta\text{-}Al_2O_3)}}{3}$$

and substituting the corresponding values to $A_i$, $B_i$, and $\chi_i$ parameters, we get for *i*-$MgGa_2O_4$

$$A_{2,av} = (2.17 \times 1 + 1.9695 \times 2)/3 = 2.036$$

$$\chi_{2,av} = (1.3 \times 1 + 1.6 \times 2)/3 = 1.5$$

$$B_{2,av} = -(2.71 + 2 \times 2.31)/3 = -2.443 \text{ eV}$$

while for *i*-$MgAl_2O_4$, we obtain

$$A_{1,av} = (2.17 \times 1 + 2.2313 \times 2)/3 = 2.211$$

$$\chi_{1,av} = (1.3 \times 1 + 1.5 \times 2)/3 = 1.433$$

$$B_{1,av} = -(2.71 + 2.225 \times 2) = -2.387 \text{ eV}$$

In Table 3, we report the band-gap values of normal and inverted double spinels for some particular compositions from which we see that a value of 6.36 eV is now obtained for the double spinel *i*-$Mg(AlGa)O_4$ having the structure: $(Al_{.5}Ga_{.5})^T(MgAl_{.5}Ga_{.5})^{Oct}O_4$.

It has been reported that, under ordinary conditions, the formation of *i*-$MgGa_2O_4$ is energetically favored with respect to *n*-$MgGa_2O_4$, whereas the contrary is true for $MgAl_2O_4$.[65] According to this, Pilania et al.[30] suggested that in the double spinel $(Ga)[MgAl]O_4$, the "local configurational environments preserve the specific coordinations of their atomic constituents coming from the two end-point single spinels", so that as end ternary oxide in Figure 5, we should use *n*-$MgAl_2O_4$. In this case, however, owing to the almost coincident value of $E_{g,opt}$ derived for *i*-$MgGa_2O_4$ (5.70 eV) and *n*-$MgGa_2O_4$ (5.67 eV), we can anticipate (also see Figure S1) that the $E_g$ values derived for the double spinel *i*-$Mg(Al_xGa_{(2-x)})O_4$ ($E_g$ = 6.76 eV) coincide with the value of 6.75 eV measured at $x = 1$ for *n*-MAGO (see Figures 5 and S1). This last value is about 0.4 eV higher than that reported (6.36 eV) for *i*-$Mg(AlGa)O_4$ (Table 3a). The difference of 0.4 eV in $E_g^{th}$ values, obtained by using the two different end terms for $MgAl_2O_4$, reflects the fact that the structure of the double spinel, at $x = 1$, is quite different as derived from the use of the structural formula $(Mg_{1-i}Al_iGa_{i-j})^T[Mg_iAl_{2-x-j}Ga_{x-i+j}]^{Oct}.O_4$, with occupancy fac-



https://doi.org/10.1021/acsorginorgau.3c00030
ACS Org. Inorg. Au 2024, 4, 120–134

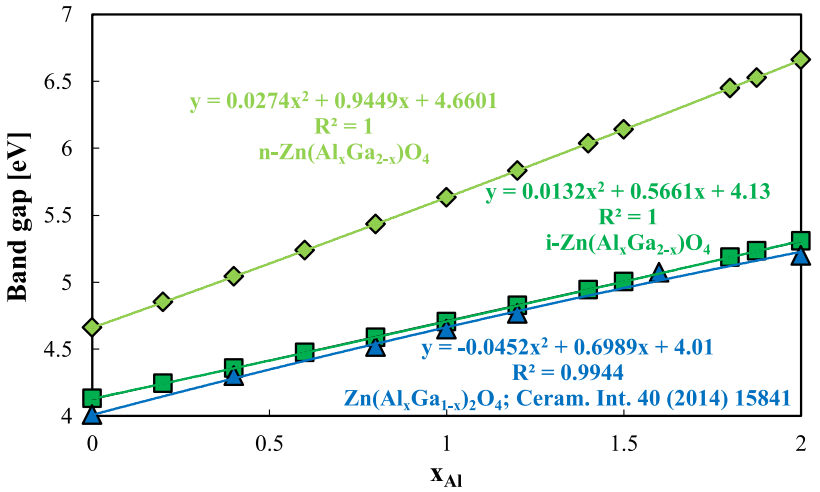


**Figure 6.** Modeling of optical band-gap values of doubles spinel $Zn(Al_xGa_{(1-x)})_2O_4$ (ZAGO) as a function of Al composition for ($i$ = 0) $n$-ZAGO (diamond) and for ($i$ = 1) $i$-ZAGO (square). Theoretical band-gap values have been derived by using eqs 9 and 9a−9d with $E_{gT2}$ = 4.67 eV, $A_{2av}$ = 1.93, $B_{2av}$ = −2.3066 eV, $\chi_{2av}$ = 1.60, $A_{1av}$ = 2.3183, $B_{1av}$ = −2.3066 eV, and $\chi_{1av}$ = 1.5333 for $n$-ZAGO and with $E_{gT2}$ = 4.13 eV, $A_{2av}$ = 1.7748, $B_{2av}$ = −2.27 eV, $\chi_{2av}$ = 1.60, $A_{1av}$ = 1.9483, $B_{1av}$ = −2.2133 eV, and $\chi_{1av}$ = 1.5333 for $i$-ZAGO. Experimental optical band-gap values (triangles) of $Zn(Al_xGa_{(1-x)})_2O_4$ samples prepared under hydrothermal conditions at 240 °C for 5 h.[34]

tors $i$ = 1 and $j$ = 0.5 in the first case ($i$-MAGO) and $i$ = 0.5, $j$ = 0 in the second case ($n$,$i$-MAGO), to which correspond the two structures $(Ga_{0.5}Al_{0.5})[Mg_1Al_{0.5\ Ga0.5}]O_4$ and $(Mg_{.5}Ga_{.5})$-$[Mg_{.5}AlGa_{.5}]O_4$, respectively.

We have to stress that the DFT band-gap value for $(Ga)[MgAl]O_4$ (3.33 eV) reported in the literature[30] and calculated by using the modified generalized gradient approximation (GGA-PBE) is much lower than the values reported above (see Table 3). We are not aware of experimental data reporting the band-gap value of such quaternary double spinel oxide, but the occupancy parameters of a single-crystal sample, having composition $Mg_{1.003}Al_{1.02}Ga_{0.978}O_4$, reported in the literature[59] suggest a very low occupancy of tetrahedral sites (3.5%) by $Al^{3+}$, a much higher occupancy (68%) by $Ga^{3+}$ ions, and a still appreciable (28.5%) presence of $Mg^{2+}$ ions in tetrahedral sites. These results agree, also, with recent findings showing a preferential distribution of $Al^{3+}$ on octahedral sites with respect to $Ga^{3+}$ in $\beta$-$AlGaO_3$ oxide,[70] while the presence of $Mg^{2+}$ ions in octahedral sites ($i$ = 0.38) has been reported recently[60] for polycrystalline samples of MAGO. From these findings, it seems reasonable to assume for the double spinel $Mg(AlGa)O_4$ an inversion parameter comprised between 0.4 and 0.7 and an occupancy factor $j$ = 0. According to this, depending on the thermal history and fabrication methods, we could expect an optical band-gap value for the $MgAlGaO_4$ double spinel at around 6.55 ± 0.2 eV. Optical band-gap values lower than 6.35 eV should be accepted with some caution and probably it could be traced to the presence of localized electronic states within the gap owing to the presence of crystallographic defects and/or impurity bands.[64]

### 3.2. $Zn(Al_xGa_{2-x})O_4$ Double Spinels: $n$,$i$-ZAGO and Quaternary Mixed Oxides $Zn_xMg_{(1-x)}(Ga_2,Al_2)O_4$

In agreement with the approach discussed above for the MAGO double spinel and by using eqs 9 with the corresponding average parameters, calculated as above, we plot in Figure 6 the optical band-gap values, for the normal double spinel $n$-ZAGO, as a function of the composition variable in the same range of composition ($0 \le x_{Al} \le 2$) previously reported for MAGO. In this case, the optical band-gap values of the end points ($x$ = 0 and $x$ = 2) coincide, for $i$ = 0, with the band-gap values of ternary spinels $n$-$ZnGa_2O_4$ (4.67 eV) and $n$-$ZnAl_2O_4$ (6.67 eV), respectively, while for $x$ = 1, a value of 5.63 eV is obtained for the $n$-$Zn(AlGa)O_4$ double spinel (see also Table 3).

In Figure 6, we also plot the optical band-gap values of the inverse ($i$ = 1) double spinel ($i$-ZAGO) by using as end terms of the quaternary oxides system the band-gap values of ternary oxides $i$-$ZnGa_2O_4$ ($E_{g,opt}$ = 4.13 eV) and $i$-$ZnAl_2O_4$ ($E_{g,opt}$ = 5.32 eV), respectively. The values of the different parameters employed for modeling the behavior of $E_{g,opt}$ vs $x_{Al}$ are reported in the caption of Figure 6.

As for the experimental optical band-gap values of the $n$-$Zn(Al_xGa_{1-x})_2O_4$ double spinel, a very wide range of values have been reported in the literature for the ternary end terms $ZnGa_2O_4$ and $ZnAl_2O_4$, as discussed in Section 3 (see Table 1), while very few data have been reported in the literature for the intermediate range of composition pertaining to the double spinel composition (see Table 3). From a close inspection of the experimental data, we can reasonably assume that single $Zn(Ga,Al)_2O_4$ or $Zn(Al_xGa_{1-x})_2O_4$ double spinels polycrystalline samples prepared by hydrothermal synthesis and lower temperatures display lower optical band-gap values with respect to their counterpart prepared by the solid-state route and/or higher temperatures. By assuming as reference values the single-crystal optical band-gap value of end terms $n$-$ZnGa_2O_4$ (4.70 ± 0.1 eV)[4,37,50] and $n$-$ZnAl_2O_4$ (6.70 ± 0.1 eV),[22,23] obtained from the Tauc plot or from photoluminescence excitation spectra (see also Table 1), we will discuss the existing experimental data of the double spinel, $Zn(Al_xGa_{1-x})_2O_4$, to evidence some incongruences and possible answers.

In Table 3, a good agreement is obtained between the estimated band-gap values of $n$-$Zn(Al_{0.2}Ga_{1.8})O_4$ and $n$-$Zn(Al_{0.5}Ga_{1.5})O_4$ double spinels and the fundamental gap of these spinel calculated by means of eq 7 and by using the experimental energy exciton peak, $E^{exc}$, values reported in Table 3. We have to mention that in both cases, the investigated samples were prepared by a solid-state method and at a high temperature. As for the $n$-$Zn(AlGa)O_4$ double spinel, a value of $E_g$ = 5.63 eV has been estimated in Figure 6 to which a fundamental gap of 6.16 eV is associated in agreement with the results of the same double spinel at lower Al content.


https://doi.org/10.1021/acsorginorgau.3c00030
ACS Org. Inorg. Au 2024, 4, 120−134

Table 4. Band-Gap Values of Quaternary Oxide Spinels Estimated by the Semiempirical Approach, $E_g^{th}$, Experimental Optical Gap Values $^{d,i}E_{exp}^{opt}$ Obtained by Tauc's Method (d: Direct; i: Indirect), Experimental Excitation Peak Energy Values of the Excitonic Gap $E_{exp}^{exc}$, Experimental Fundamental Band Gap, $E_f^{exp}$, Obtained (through eq 6 and 7) from $E_{exp}^{exc}$ or $E_{exp}^{opt}$, and Theoretical $E_f^{th}$ Obtained (through eqs 6 and 7) from $E_g^{th,opt}$

| phase | $E_g^{th}$ [eV] | $E_{exp}^{opt}$ [eV] | $E_{exp}^{exc}$ [eV] | $E_g$ (DFT) [eV] | $E_f^{exp}$ [eV] | $E_f^{th}$ [eV] |
|---|---|---|---|---|---|---|
| $Zn_{0.25}Mg_{0.75}Ga_2O_4$ | 5.44 | | 5.23[41] | | 5.45 | |
| $Zn_{0.5}Mg_{0.5}Ga_2O_4$ | 5.175 | 4.75[37] | 5.05[41] | | 5.25[41] | |
| | | | | | 5.20[37] | |
| $\gamma-(Zn_{0.5}Mg_{0.5})Al_2O_4$ | 6.13 | 5.52[73] | | | 6.04 | |
| $\gamma$-$Zn_{0.25}Mg_{0.75}Ga_2O_4$ | 5.043 | | 5.23[41] | | 5.45 | 5.52 |
| $\gamma$-$Zn_{0.5}Mg_{0.5}Ga_2O_4$ | 4.80 | 4.75[37] | 5.05[41] | | 5.25[41] | 5.25 |
| | | | | | 5.2[37] | |

In Figure 6, we also plotted the experimental optical band-gap values of the solid solution $Zn(Al_xGa_{1-x})_2O_4$, covering all of the ranges of composition[34] and prepared under similar hydrothermal conditions. As shown in Figure 6, the experimental optical band-gap values are in very good agreement with the theoretical data points of $i$-$Zn(Al_xGa_{1-x})_2O_4$ calculated by using ternary end terms $i$-$ZnGa_2O_4$ and $i$-$ZnAl_2O_4$.

By excluding the formation of $i$-$Zn(Al_xGa_{1-x})_2O_4$ ($i_{exp}$ < 0.06), the lower optical band-gap values of Figure 6 could be attributed to the presence of crystallographic defects or to the formation of an impurity band in $n$-$Zn(Al_xGa_{1-x})_2O_4$ related to the preparation method. We like to mention that the formation of antisite defects, $Zn_{Ga}$, as well as the formation of a polaronic band in the presence of an excess of Zn, with respect to the stoichiometric ratio $Zn/(Ga_{(1-x)}Al_x) = 0.5$, energetically located at about 0.5−0.9 eV above the valence band of $n$-ZGO, have been reported in the literature.[52,72]

However, we like to stress that a good agreement between the $E_g^{th}$ values of Zn(AlGa)$O_4$ and the direct optical band gap of samples prepared under hydrothermal conditions is obtained (see Tables 3 and 4) by modeling the quaternary mixed oxides by using the two ternary oxide systems wz-ZnO/$\gamma$-$Ga_2O_3$ and wz-ZnO/$\gamma$-$Al_2O_3$. Both $\gamma$-$Al_2O_3$ and $\gamma$-$Ga_2O_3$ crystallize as defective cubic spinel ($\gamma$-$Al_2O_{2.73}$ and $\gamma$-$Ga_2O_{2.73}$), and the formation of a cubic spinel solid solution $\gamma$-$Zn(Al_xGa_{2-x})O_4$, at much lower temperatures than those employed in the solid-state route of preparation of spinels, could offer an alternative explanation for the behavior of samples of $Zn(Al_xGa_{(1-x)})_2O_4$ prepared under hydrothermal conditions. This last hypothesis could explain the behavior of the experimental data set depicted in Figure 6 as well as the good agreement between the $E_g$ value derived for the quaternary mixed oxide $\gamma$-Zn(AlGa)$O_4$, through our semiempirical approach, and the $E_f$ values, estimated by means of eqs 6 and 7, by using the $E_{g,opt}$ values reported for Zn(AlGa)$O_4$ samples in the literature.[71]

As for the quaternary oxides having a cubic spinel crystalline structure, we report, in Table 4, the experimental exciton peak energy or the optical band-gap values of the quaternary mixed oxides $(Zn_{1-x}Mg_x)Ga_2O_4$, prepared by a solid-state route at high temperatures ($T$ = 1200 °C, 8 h) for $x$ = 0.25, or as a single crystal at $x$ = 0.5. By using eqs 6−7, we estimated the fundamental gap, $E_f$, of both samples, which almost coincides with the band-gap values of the quaternary oxides estimated by our approach by assuming as end terms, of these quaternary oxides, the ternary spinels $n$-$ZnGa_2O_4$ and $n$-$MgGa_2O_4$ (or $i$-$MgGa_2O_4$). It is interesting to note that the fundamental gap of both quaternary samples can also be reasonably fitted by using as end terms of quaternary oxides the ternary systems wtz-(ZnO,MgO)/$\gamma$-$Ga_2O_3$ and wtz-(ZnO,MgO)/$\gamma$-$Al_2O_3$. Both gallia and alumina $\gamma$-polymorphs crystallize as defective cubic spinels, while as for ZnO and MgO oxides, we used the wurtzite phase by assuming that in the quaternary oxide with a cubic spinel structure, both cations occupy tetrahedrally coordinated sites. This assumption is particularly stringent for the good fitting of the fundamental gap of the $Zn_{.5}Mg_{.5}Al_2O_4$ sample prepared by a low-temperature hydrothermal route and subsequent thermal treatment at 800 °C for 4 h.

## 4. CONCLUSIONS

A detailed investigation of the modeling procedure of band-gap values of normal ($i$ = 0) and complex ($i$ < 1) cubic spinels $MgAl_2O_4$, $MgGa_2O_4$, $ZnAl_2O_4$, and $Zn(Al_2,Ga_2)O_4$ has been carried by using a semiempirical approach based on the correlation between the band gap of oxides and the difference of average electronegativity of metallic cations ($\chi_{av}$) and oxygen recently derived for ternary and quaternary mixed oxides. The extension of the correlation to the different polymorphs and mixed ternary or quaternary oxides, initially derived for binary oxides, has been successfully tested also for the complex investigated spinel structures. The band-gap values of $MgAl_2O_4$ and $MgGa_2O_4$ spinels derived, according to our approach, agree nicely with the values reported in the literature for both compounds.

In the case of bulk $n$-$ZnAl_2O_4$, our band-gap estimate ($E_g$ = 6.67 eV) was in very good agreement with the fundamental gap ($E_f$ = 6.62 eV) of bulk samples, derived by using the direct optical gap measured by Tauc's method, whereas powder samples of ZAO displayed higher (7.28 eV) fundamental gap values, derived by using the exciton energy peak values reported in the literature. The larger values of $E_f$ have been attributed to the possible onset of quantum size effects, as reported in the literature for spinel samples having smaller grain sizes. At variance with the above-described behavior, in the case of the $n$-$ZnGa_2O_4$ spinel, the band gap estimated by us ($E_g$ = 4.67 eV) was in good agreement with the optical band-gap values reported in the literature but about 0.5 eV lower than the fundamental gap, derived from the exciton energy peak values reported in the literature or estimated by spectroscopy ellipsometry.

In the case of inverse spinels, the few experimental data and the absence of information on the inversion degree of the few investigated systems did not allow an extensive check of our estimated band-gap values. However, we have to mention that for some partially inverted spinels of $MgGa_2O_4$ ($i$ = 0.44) and $ZnGa_2O_4$ ($i$ < 0.30), a quite good agreement between our band-gap estimate and the experimental band-gap values was observed. In many cases, our estimates of spinel band-gap values have shown a better agreement with respect to the


https://doi.org/10.1021/acsorginorgau.3c00030
ACS Org. Inorg. Au 2024, 4, 120−134

estimates provided by first-principles and DFT-based techniques.

The band-gap values of double spinels $n$-$Zn(Al_xGa_{1-x})O_4$ and quaternary oxides, of general formula $Zn_xMg_{1-x}Al_2O_4$, estimated by using the fitting equations derived[9] for quaternary alumina garnets, displayed a very good agreement with the fundamental band-gap values reported in the literature. Further experimental investigations aimed at explaining the observed discrepancies are welcome for reaching a deeper understanding of the influence of the preparation method on the solid-state properties of these technologically important materials. However, the results of this work confirm that the semiempirical approach to the band-gap modeling of mixed oxides, proposed by the present authors, is, in many cases, able to derive the right information on the expected band gap of mixed oxides, provided that the restrictions embodied in the model are satisfied.

## ■ ASSOCIATED CONTENT

### Data Availability Statement

The data underlying this study are available in the published article and its Supporting Information.

### Supporting Information

The Supporting Information is available free of charge at https://pubs.acs.org/doi/10.1021/acsorginorgau.3c00030.

MAGO band-gap data and $A$ and $B$ parameters for binary oxides (PDF)

## ■ AUTHOR INFORMATION


### Corresponding Author

**Francesco Di Quarto** − *Dipartimento di Ingegneria, Università degli Studi di Palermo, 90128 Palermo, Italy;* orcid.org/0000-0001-8751-5928; Email: francesco.diquarto@unipa.it

### Authors

**Andrea Zaffora** − *Dipartimento di Ingegneria, Università degli Studi di Palermo, 90128 Palermo, Italy;* orcid.org/0000-0002-4185-8308

**Francesco Di Franco** − *Dipartimento di Ingegneria, Università degli Studi di Palermo, 90128 Palermo, Italy;* orcid.org/0000-0002-5722-2881

**Monica Santamaria** − *Dipartimento di Ingegneria, Università degli Studi di Palermo, 90128 Palermo, Italy;* orcid.org/0000-0002-8690-4881

Complete contact information is available at: https://pubs.acs.org/10.1021/acsorginorgau.3c00030


### Notes

The authors declare no competing financial interest.

## ■ ACKNOWLEDGMENTS

The authors thank M. Rita Cinà for her support in providing many of the articles cited in the References section and the University of Palermo for the financial support.

## ■ REFERENCES


(1) Zhao, Q.; Yan, Z.; Chen, C.; Chen, J. Spinels: Controlled Preparation, Oxygen Reduction/Evolution Reaction Application, and Beyond. *Chem. Rev.* **2017**, *117* (15), 10121−10211.

(2) Nørskov, J. K.; Bligaard, T.; Rossmeisl, J.; Christensen, C. H. Towards the Computational Design of Solid Catalysts. *Nat. Chem.* **2009**, *1* (1), 37−46.

(3) Dillert, R.; Taffa, D. H.; Wark, M.; Bredow, T.; Bahnemann, D. W. Research Update: Photoelectrochemical Water Splitting and Photocatalytic Hydrogen Production Using Ferrites (MFe2O4) under Visible Light Irradiation. *APL Mater.* **2015**, *3* (10), No. 104001.

(4) Chikoidze, E.; Sartel, C.; Madaci, I.; Mohamed, H.; Vilar, C.; Ballesteros, B.; Belarre, F.; Del Corro, E.; Vales-Castro, P.; Sauthier, G.; Li, L.; Jennings, M.; Sallet, V.; Dumont, Y.; Pérez-Tomás, A. P-Type Ultrawide-Band-Gap Spinel ZnGa2O4: New Perspectives for Energy Electronics. *Cryst. Growth Des.* **2020**, *20* (4), 2535−2546.

(5) Kao, Y. N.; Huang, W. L.; Chang, S. P.; Lai, W. C.; Chang, S. J. Investigation of Different Oxygen Partial Pressures on MgGa2O4-Resistive Random-Access Memory. *ACS Omega* **2023**, *8*, 3705−3712.

(6) Bortz, M. L.; French, R. H. Optical Reflectivity Measurements Using a Laser Plasma Light Source. *Appl. Phys. Lett.* **1989**, *55* (19), 1955−1957.

(7) Feldbach, E.; Kudryavtseva, I.; Mizohata, K.; Prieditis, G.; Räisänen, J.; Shablonin, E.; Lushchik, A. Optical Characteristics of Virgin and Proton-Irradiated Ceramics of Magnesium Aluminate Spinel. *Opt. Mater.* **2019**, *96*, No. 109308.

(8) Rojas-Hernandez, R. E.; Rubio-Marcos, F.; Romet, I.; Del Campo, A.; Gorni, G.; Hussainova, I.; Fernandez, J. F.; Nagirnyi, V. Deep-Ultraviolet Emitter: Rare-Earth-Free ZnAl2O4Nanofibers via a Simple Wet Chemical Route. *Inorg. Chem.* **2022**, *61* (30), 11886−11896.

(9) Di Quarto, F.; Zaffora, A.; Di Franco, F.; Santamaria, M. Band Gap Modeling of Different Ternary and Quaternary Alumina Garnet Phases Y3(AlxGa1−x)5O12 (YAGG) and Lu3(AlxGa1−x)5O12 (LuAGG). A Semiempirical Approach. *J. Phys. Chem. C* **2022**, *126* (40), 17313−17327.

(10) Di Quarto, F.; Zaffora, A.; Di Franco, F.; Santamaria, M. A Generalized Semiempirical Approach to the Modeling of the Optical Band Gap of Ternary Al-(Ga, Nb, Ta, W) Oxides Containing Different Alumina Polymorphs. *Inorg. Chem.* **2021**, *60* (3), 1419−1435.

(11) Di Quarto, F.; Sunseri, C.; Piazza, S.; Romano, M. C. Semiempirical Correlation between Optical Band Gap Values of Oxides and the Difference of Electronegativity of the Elements. Its Importance for a Quantitative Use of Photocurrent Spectroscopy in Corrosion Studies. *J. Phys. Chem. B* **1997**, *101* (97), 2519−2525.

(12) Di Quarto, F.; Zaffora, A.; Di Franco, F.; Santamaria, M. Review — Photocurrent Spectroscopy in Corrosion and Passivity Studies: A Critical Assessment of the Use of Band Gap Value to Estimate the Oxide Film Composition. *J. Electrochem. Soc.* **2017**, *164* (12), C671−C681.

(13) Di Quarto, F.; Di Franco, F.; Zaffora, A.; Santamaria, M. Photocurrent Spectroscopy in Passivity Studies. In *Encyclopedia of Interfacial Chemistry: Surface Science and Electrochemistry*; Wandelt, K., Ed.; Elsevier Inc, 2018; Vol. *1*, pp 361−371.

(14) Pauling, L. *The Nature of Chemical Bond*; Cornell University Press: Ithaca, NY, 1959.

(15) Phillips, J. C. *Bonds and Bands in Semiconductors*; Academic Press: New York, 1973.

(16) Chandran, C. V.; Kirschhock, C. E. A.; Radhakrishnan, S.; Taulelle, F.; Martens, J. A.; Breynaert, E. Alumina: Discriminative Analysis Using 3D Correlation of Solid-State NMR Parameters. *Chem. Soc. Rev.* **2019**, *48* (1), 134−156.

(17) Schleife, A.; Fuchs, F.; Furthmüller, J.; Bechstedt, F. First-Principles Study of Ground- and Excited-State Properties of MgO, ZnO, and CdO Polymorphs. *Phys. Rev. B* **2006**, *73* (24), No. 245212.

(18) Fan, X. F.; Sun, H. D.; Shen, Z. X.; Kuo, J. L.; Lu, Y. M. A First-Principle Analysis on the Phase Stabilities, Chemical Bonds and Band Gaps of Wurtzite Structure Alloys(A = Ca, Cd, Mg). *J. Phys.: Condens. Matter* **2008**, *20* (23), No. 235221.

(19) Koster, R. S.; Fang, C. M.; Dijkstra, M.; Van Blaaderen, A.; Van Huis, M. A. Stabilization of Rock Salt ZnO Nanocrystals by Low-Energy Surfaces and Mg Additions: A First-Principles Study. *J. Phys. Chem. C* **2015**, *119* (10), 5648−5656.

(20) *CRC Handbook of Chemistry and Physics*, 90th ed.; Lide, D. R., Ed.; CRC Press/Taylor and Francis: Boca Raton, 2010.
(21) Di Quarto, F.; Zaffora, A.; Di Franco, F.; Santamaria, M. Review - Photocurrent Spectroscopy in Corrosion and Passivity Studies: A Critical Assessment of the Use of Band Gap Value to Estimate the Oxide Film Composition. *J. Electrochem. Soc.* **2017**, *164* (12), C671−C681.
(22) Kominami, H.; Iguchi, T.; Nakanishi, Y.; Hara, K. Ultra-Violet Emission of Aluminates Phosphors Prepared by Solid Phase Synthesis. *J. Adv. Res. Phys.* **2011**, *2* (2), No. 021109.
(23) Ishinaga, T.; Iguchi, T.; Kominami, H.; Hara, K.; Kitaura, M.; Ohnishi, A. Luminescent Property and Mechanism of ZnAl2O4 Ultraviolet Emitting Phosphor. *Phys. Status Solidi (C)* **2015**, *12* (6), 797−800.
(24) Kominami, H.; Sonoda, N.; Hara, K. Preparation and Luminescent Characteristics of UV-C Emitting ZnAl2O4 Phosphor for Sterilization Device. *Proc. Int. Disp. Workshops* **2020**, No. 346, DOI: 10.36463/idw.2020.0346.
(25) Belyaev, A. V.; Evdokimov, I. I.; Drobotenko, V. V.; Sorokin, A. A. A New Approach to Producing Transparent ZnAl2O4 Ceramics. *J. Eur. Ceram Soc.* **2017**, *37* (7), 2747−2751.
(26) Prieditis, G.; Feldbach, E.; Kudryavtseva, I.; Popov, A. I.; Shablonin, E.; Lushchik, A. Luminescence Characteristics of Magnesium Aluminate Spinel Crystals of Different Stoichiometry. *IOP Conf. Ser.: Mater. Sci. Eng.* **2019**, *503*, No. 012021.
(27) Museur, L.; Feldbach, E.; Kotlov, A.; Kitaura, M.; Kanaev, A. Donor-Acceptor Pair Transitions in MgAl2O4 Spinel. *J. Lumin.* **2024**, *265*, No. 120235.
(28) Mo, S. Di.; Ching, W. Electronic Structure of Normal, Inverse, and Partially Inverse Spinels in the MgAl2O4 System. *Phys. Rev. B* **1996**, *54* (23), No. 16555.
(29) Reshak, A. H.; Khan, S. A.; Alahmed, Z. A. Investigation of Electronic Structure and Optical Properties of MgAl2O4: DFT Approach. *Opt. Mater.* **2014**, *37*, 322−326.
(30) Pilania, G.; Kocevski, V.; Valdez, J. A.; Kreller, C. R.; Uberuaga, B. P. Prediction of Structure and Cation Ordering in an Ordered Normal-Inverse Double Spinel. *Commun. Mater.* **2020**, *1* (1), No. 84.
(31) Hosseini, S. M. Structural, Electronic and Optical Properties of Spinel MgAl2O4 Oxide. *Phys. Status Solidi (B)* **2008**, *245* (12), 2800−2807.
(32) Amin, B.; Khenata, R.; Bouhemadou, A.; Ahmad, I.; Maqbool, M. Opto-Electronic Response of Spinels MgAl2O4 and MgGa2O4 through Modified Becke-Johnson Exchange Potential. *Phys. B* **2012**, *407* (13), 2588−2592.
(33) Dixit, H.; Tandon, N.; Cottenier, S.; Saniz, R.; Lamoen, D.; Partoens, B.; Van Speybroeck, V.; Waroquier, M. Electronic Structure and Band Gap of Zinc Spinel Oxides beyond LDA: ZnAl2O4, ZnGa2O4 and ZnIn2O4. *New J. Phys.* **2011**, *13* (6), No. 063002.
(34) Sakoda, K.; Hirano, M. Formation of Complete Solid Solutions, Zn(AlxGa1−x)2O4 Spinel Nanocrystals via Hydrothermal Route. *Ceram. Int.* **2014**, *40* (10), 15841−15848.
(35) Anand, G. T.; Kennedy, L. J.; Vijaya, J. J.; Kaviyarasan, K.; Sukumar, M. Structural, Optical and Magnetic Characterization of Zn1−xNixAl2O4 ($0 \leq x \leq 5$) Spinel Nanostructures Synthesized by Microwave Combustion Technique. *Ceram. Int.* **2015**, *41* (1), 603−615.
(36) Oliveira, M. C.; Ribeiro, R. A. P.; Longo, E.; Bomio, M. R. D.; de Lázaro, S. R. Quantum Mechanical Modeling of Zn-Based Spinel Oxides: Assessing the Structural, Vibrational, and Electronic Properties. *Int. J. Quantum Chem.* **2020**, *120* (22), No. e26368.
(37) Galazka, Z.; Ganschow, S.; Irmscher, K.; Klimm, D.; Albrecht, M.; Schewski, R.; Pietsch, M.; Schulz, T.; Dittmar, A.; Kwasniewski, A.; Grueneberg, R.; Anooz, S.; Bin; Popp, A.; Juda, U.; Hanke, I. M.; Schroeder, T.; Bickermann, M. Bulk Single Crystals of $\beta$-Ga2O3 and Ga-Based Spinels as Ultra-Wide Bandgap Transparent Semiconducting Oxides. *Prog. Cryst. Growth Charact. Mater.* **2021**, *67* (1), No. 100511.
(38) Sommer, S.; Bøjesen, E. D.; Reardon, H.; Iversen, B. B. Atomic Scale Design of Spinel ZnAl2O4 Nanocrystal Synthesis. *Cryst. Growth Des.* **2020**, *20* (3), 1789−1799.
(39) Liu, Z.; Hu, P.; Jing, X.; Wang, L. Luminescence of Native Defects in MgGa2O4. *J. Electrochem. Soc.* **2009**, *156* (1), No. H43.
(40) Basavaraju, N.; Sharma, S.; Bessière, A.; Viana, B.; Gourier, D.; Priolkar, K. R. Red Persistent Luminescence in MgGa2O4: Cr3+; a New Phosphor for in Vivo Imaging. *J. Phys. D: Appl. Phys.* **2013**, *46* (37), No. 375401.
(41) Luchechko, A.; Kravets, O. Novel Visible Phosphors Based on MgGa2O4-ZnGa2O4 Solid Solutions with Spinel Structure Co-Doped with Mn2+ and Eu3+ Ions. *J. Lumin.* **2017**, *192*, 11−16.
(42) Can, M. M.; Jaffari, G. H.; Aksoy, S.; Shah, S. I.; Firat, T. Synthesis and Characterization of ZnGa2O4 Particles Prepared by Solid State Reaction. *J. Alloys Compd.* **2013**, *549*, 303−307.
(43) Oshima, T.; Niwa, M.; Mukai, A.; Nagami, T.; Suyama, T.; Ohtomo, A. Epitaxial Growth of Wide-Band-Gap ZnGa2O4 Films by Mist Chemical Vapor Deposition. *J. Cryst. Growth* **2014**, *386*, 190−193.
(44) Omata, T.; Ueda, N.; Ueda, K.; Kawazoe, H. New Ultraviolet-transport Electroconductive Oxide, ZnGa2O4 Spinel. *Appl. Phys. Lett.* **1994**, *64* (9), 1077−1078.
(45) Galazka, Z.; Ganschow, S.; Schewski, R.; Irmscher, K.; Klimm, D.; Kwasniewski, A.; Pietsch, M.; Fiedler, A.; Schulze-Jonack, I.; Albrecht, M.; Schröder, T.; Bickermann, M. Ultra-Wide Bandgap, Conductive, High Mobility, and High Quality Melt-Grown Bulk ZnGa 2 O 4 Single Crystals. *APL Mater.* **2019**, *7* (2), No. 022512, DOI: 10.1063/1.5053867.
(46) Zou, L.; Xiang, X.; Wei, M.; Li, F.; Evans, D. G. Single-Crystalline ZnGa2O4 Spinel Phosphor via a Single-Source Inorganic Precursor Route. *Inorg. Chem.* **2008**, *47* (4), 1361−1369.
(47) Singh, A. K.; Chen, P. W.; Wuu, D. S. Growth and Characterization of Co-Sputtered Al-Doped ZnGa2O4 Films for Enhancing Deep-Ultraviolet Photoresponse. *Appl. Surf. Sci.* **2021**, *566*, No. 150714.
(48) Can, M. M.; Akbaba, Y.; Shawuti, S.; Kaneko, S. Blue Shift in Optical Emission Spectra of ZnGa2O4 by Lattice Deformation Due to Eu Atom Amount in Spinel Lattice. *Appl. Phys. A* **2022**, *128* (12), No. 1041.
(49) Li, X.; Chen, T. P.; Liu, P.; Liu, Y.; Leong, K. C.; Pearton, S. J.; Norton, D. P.; Ip, K.; Heo, Y. W.; Steiner, T.; Özgür, U.; Alivov, Y. I.; Liu, C.; Teke, A.; Reshchikov, M. A.; Dogan, S.; Avrutin, V.; Cho, S.; Morkoc, H.; Reynolds, D. C.; Look, D. C.; Jogai, B.; Nie, J. C.; Yang, J. Y.; Piao, Y.; Li, H.; Sun, Y.; Xue, Q. M.; Xiong, C. M.; Dou, R. F.; Tu, Q. Y. Effects of Free Electrons and Quantum Confinement in Ultrathin ZnO Films: A Comparison between Undoped and Al-Doped ZnO. *Opt. Express* **2013**, *21* (12), 14131−14138.
(50) Noto, L. L.; Mbongo, M. Photoluminescence and Thermoluminescence Properties of ZnGa2O4 Prepared by a Microwave Assisted Solid State Reaction. *Phys. B* **2020**, *578*, No. 411768.
(51) Jeong, I. K.; Park, H. L.; Mho, S.-i. Photoluminescence of ZnGa2O4Mixed with InGaZnO4. *Solid State Commun.* **1998**, *105* (3), 179−183.
(52) Sabino, F. P.; Chatratin, I.; Janotti, A.; Dalpian, G. M. Hole Conductivity through a Defect Band in ZnGa2O4. *Phys. Rev. Mater.* **2022**, *6*, No. 064602.
(53) Hilfiker, M.; Stokey, M.; Korlacki, R.; Kilic, U.; Galazka, Z.; Irmscher, K.; Zollner, S.; Schubert, M. Zinc Gallate Spinel Dielectric Function, Band-to-Band Transitions, and Γ-Point Effective Mass Parameters. *Appl. Phys. Lett.* **2021**, *118* (13), No. 132102.
(54) Yi, Z.; Liu, P.; Xu, Y. Multimode Dynamic Photoluminescence of Bi3+-Activated ZnGa2O4 for Optical Information Encryption. *Inorg. Chem.* **2023**, *62* (24), 9671−9678.
(55) Pathak, N.; Ghosh, P. S.; Saxena, S.; Dutta, D.; Yadav, A. K.; Bhattacharyya, D.; Jha, S. N.; Kadam, R. M. Exploring Defect-Induced Emission in ZnAl2O4: An Exceptional Color-Tunable Phosphor Material with Diverse Lifetimes. *Inorg. Chem.* **2018**, *57* (7), 3963−3982.
(56) Dorenbos, P. Charge Transfer Bands in Optical Materials and Related Defect Level Location. *Opt. Mater.* **2017**, *69*, 8−22.
(57) Ueda, J.; Dorenbos, P.; Bos, A. J. J.; Kuroishi, K.; Tanabe, S. Control of Electron Transfer between Ce3+ and Cr3+ in the Y3Al5−

xGaxO12 Host via Conduction Band Engineering. *J. Mater. Chem. C* **2015**, *3* (22), 5642−5651.
(58) Ueda, J.; Meijerink, A.; Dorenbos, P.; Bos, A. J. J.; Tanabe, S. Thermal Ionization and Thermally Activated Crossover Quenching Processes for 5d-4f Luminescence in Y3Al5-XGaxO12:Pr3+. *Phys. Rev. B* **2017**, *95* (1), No. 014303.
(59) Ito, T.; Nakatsuka, A.; Maekawa, H.; Yoshiasa, A.; Yamanaka, T. Site Preference of Cations and Structural Variation in MgAl2-XGaxO4 ($0 \leq x \leq 2$) Spinel Solid Solution. *Z. Anorg. Allg. Chem.* **2000**, *626* (1), 42−49.
(60) O'Quinn, E. C.; Shamblin, J.; Perlov, B.; Ewing, R. C.; Neuefeind, J.; Feygenson, M.; Gussev, I.; Lang, M. Inversion in Mg1-XNixAl2O4 Spinel: New Insight into Local Structure. *J. Am. Chem. Soc.* **2017**, *139* (30), 10395−10402.
(61) Mathur, S.; Veith, M.; Haas, M.; Shen, H.; Lecerf, N.; Huch, V.; Hufner, S.; Haberkorn, R.; Beck, H. P.; Jilavi, M. Single-Source Sol−Gel Synthesis of Nanocrystalline ZnAl2O4:Structural and Optical Properties. *J. Am. Ceram. Soc.* **2001**, *84* (9), 1921−1928.
(62) Wang, S. F.; Sun, G. Z.; Fang, L. M.; Lei, L.; Xiang, X.; Zu, X. T. A Comparative Study of ZnAl2O4 Nanoparticles Synthesized from Different Aluminum Salts for Use as Fluorescence Materials. *Sci. Rep.* **2015**, *5*, No. 12849.
(63) Hou, Q.; Liu, K.; Chen, X.; Yang, J.; Ai, Q.; Cheng, Z.; Zhu, Y.; Li, B.; Liu, L.; Shen, D. Effects of Mg Component Ratio on Photodetection Performance of MgGa2O4 Solar-Blind Ultraviolet Photodetectors. *Phys. Status Solidi RRL* **2022**, *16* (8), No. 2200137, DOI: 10.1002/pssr.202200137.
(64) Pathak, N.; Ghosh, P. S.; Gupta, S. K.; Mukherjee, S.; Kadam, R. M.; Arya, A. An Insight into the Various Defects-Induced Emission in MgAl2O4 and Their Tunability with Phase Behavior: Combined Experimental and Theoretical Approach. *J. Phys. Chem. C* **2016**, *120* (7), 4016−4031.
(65) Kocevski, V.; Pilania, G.; Uberuaga, B. P. High-Throughput Investigation of the Formation of Double Spinels. *J. Mater. Chem. A* **2020**, *8* (48), 25756−25767.
(66) Shea, L. E.; Datta, R. K.; Brown, J. J. Photoluminescence of Mn2+-Activated ZnGa2O4. *J. Electrochem. Soc.* **1994**, *141* (7), 1950−1954.
(67) Horng, R. H.; Huang, C. Y.; Ou, S. L.; Juang, T. K.; Liu, P. L. Epitaxial Growth of ZnGa2O4: A New, Deep Ultraviolet Semiconductor Candidate. *Cryst. Growth Des.* **2017**, *17* (11), 6071−6078.
(68) Spencer, J. A.; Mock, A. L.; Jacobs, A. G.; Schubert, M.; Zhang, Y.; Tadjer, M. J. A Review of Band Structure and Material Properties of Transparent Conducting and Semiconducting Oxides: Ga2O3, Al2O3, In2O3, ZnO, SnO2, CdO, NiO, CuO, and Sc2O3. *Appl. Phys. Rev.* **2022**, *9* (1), No. 011315, DOI: 10.1063/5.0078037.
(69) Glasser, L. Solid-State Energetics and Electrostatics: Madelung Constants and Madelung Energies. *Inorg. Chem.* **2012**, *51* (4), 2420−2424.
(70) Cook, D. S.; Hooper, J. E.; Dawson, D. M.; Fisher, J. M.; Thompsett, D.; Ashbrook, S. E.; Walton, R. I. Synthesis and Polymorphism of Mixed Aluminum-Gallium Oxides. *Inorg. Chem.* **2020**, *59*, 3805−3816, DOI: 10.1021/ACS.INORGCHEM.9B03459.
(71) Sakoda, K.; Hirano, M. Effect of Heat-Treatment and Composition on Structure and Luminescence Properties of Spinel-Type Solid Solution Nanocrystals. *J. Nanosci. Nanotechnol.* **2015**, *15* (8), 6069−6077.
(72) De Vos, A.; Lejaeghere, K.; Vanpoucke, D. E. P.; Joos, J. J.; Smet, P. F.; Hemelsoet, K. First-Principles Study of Antisite Defect Configurations in ZnGa2O4:Cr Persistent Phosphors. *Inorg. Chem.* **2016**, *55* (5), 2402−2412.
(73) Saleem, M.; Varshney, D. Influence of Transition Metal Cr2+ Doping on Structural, Electrical and Optical Properties of Mg-Zn Aluminates. *J. Alloys Compd.* **2017**, *708*, 397−403.


https://doi.org/10.1021/acsorginorgau.3c00030
*ACS Org. Inorg. Au* 2024, 4, 120−134